

# Non-universal Critical Quantities from Variational Perturbation Theory and Their Application to the BEC Temperature Shift

Boris Kastening\*  
*Institut für Theoretische Physik*  
*Freie Universität Berlin*  
 Arnimallee 14  
 D-14195 Berlin  
 Germany

(Dated: June 1, 2004)

For an  $O(N)$  symmetric scalar field theory with Euclidean action  $\int d^3x [\frac{1}{2}|\nabla\phi|^2 + \frac{1}{2}r\phi^2 + \frac{1}{4!}u\phi^4]$ , where  $\phi = (\phi_1, \dots, \phi_N)$  is a vector of  $N$  real field components, variational perturbation theory through seven loops is employed for  $N = 0, 1, 2, 3, 4$  to compute the renormalized value of  $r/(N+2)u^2$  at the phase transition. Its exact large- $N$  limit is determined as well. We also extend an earlier computation of the interaction-induced shift  $\Delta\langle\phi^2\rangle/Nu$  for  $N = 1, 2, 4$  to  $N = 0, 3$ . For  $N = 2$ , the results for the two quantities are used to compute the second-order shift of the condensation temperature of a dilute Bose gas, both in the homogenous case and for the wide limit of a harmonic trap. Our results are in agreement with earlier Monte Carlo simulations for  $N = 1, 2, 4$ . The appendix contains previously unpublished numerical seven-loop data provided to us by B. Nickel.

PACS numbers: 03.75.Hh, 05.30.Jp, 12.38.Cy

## I. INTRODUCTION

Since the first experimental realizations of Bose-Einstein condensation (BEC) in dilute atomic gases [1], the preparation of such quantum gases has been achieved in many laboratories around the globe. With the continuous improvement of experimental control over these gases, it appears to be only a matter of time until precision measurements of physical quantities such as the condensation temperature, the number of bosons, and the density profile of the gas will be possible. The relations between these quantities were explored in many theoretical papers, often contradicting each other. However, after an intense investigation of the subject using Monte-Carlo simulations and various methods of field theory, most theorists agree by now that the shift  $\Delta T_c \equiv T_c - T_0$  of the condensation temperature away from its ideal gas value

$$T_0 = \frac{2\pi}{m} \left[ \frac{n}{\zeta(\frac{3}{2})} \right]^{2/3}, \quad (1)$$

where  $n$  is the particle number density and  $m$  the mass of the bosons, and where we work throughout in units where  $k_B = \hbar = 1$ , has, for a dilute homogenous Bose gas, the form [2–4]

$$\frac{\Delta T_c}{T_0} = \bar{c}_1 a n^{1/3} + [\bar{c}'_2 \ln(a n^{1/3}) + \bar{c}''_2](a n^{1/3})^2 + \dots \quad (2)$$

Here  $a$  is the  $s$ -wave scattering length corresponding to the two-particle interaction potential of the bosons and  $\bar{c}_1$ ,  $\bar{c}'_2$  and  $\bar{c}''_2$  are constants. For a comparison of several

approaches to compute  $\Delta T_c$  for the homogenous gas, the reader is referred to the recent review [5].

While the shift above is expressed in terms of the number density of bosons, the shift of  $T_c$  for a gas in the wide limit of a harmonic trap is conventionally expressed in terms of the total number  $N_b$  of bosons in the trap. With the size of the unperturbed ground state given by

$$l_{\text{ho}} = \frac{1}{\sqrt{m(\omega_x \omega_y \omega_z)^{1/3}}}, \quad (3)$$

where  $\omega_x$ ,  $\omega_y$ ,  $\omega_z$  are the frequencies characterizing the harmonic trap, the transition temperature may be written as

$$T_0 = \left( \frac{N_b}{\zeta(3)} \right)^{1/3} \frac{1}{m l_{\text{ho}}^2}, \quad (4)$$

so that the corresponding thermal wavelength  $\lambda_0 = \sqrt{2\pi/mT_0}$  becomes

$$\lambda_0 = \sqrt{2\pi} \left( \frac{N_b}{\zeta(3)} \right)^{-1/6} l_{\text{ho}}. \quad (5)$$

The equivalent of the expansion (2) is then [6, 7]

$$\frac{\Delta T_c}{T_0} = \check{c}_1 \frac{a}{\lambda_0} + \left( \check{c}'_2 \ln \frac{a}{\lambda_0} + \check{c}''_2 \right) \left( \frac{a}{\lambda_0} \right)^2 + \dots \quad (6)$$

with constants  $\check{c}_1$ ,  $\check{c}'_2$  and  $\check{c}''_2$ . The result (6) is strictly valid only in the limit of an infinitely wide trap. In this case, however, the gas is locally homogenous and the result (2) is applicable as well, if  $n$  is taken to be the central density [7, 8]. The fact that  $\Delta T_c$  is different in both cases is no contradiction, since different quantities are kept fixed, namely  $n$  in the homogenous case and  $N_b$  in the case of a wide trap. In particular,  $\bar{c}_1 > 0$ ,

\*Electronic address: boris.kastening@physik.fu-berlin.de

while  $\check{c}_1 < 0$ . Keeping  $T_c$  fixed instead, this means that, for small  $a$ , more particles have to be put into the trap as compared to the ideal gas, but at the same time the central density is reduced.

The starting point for deriving the expansions (2) and (6) is to describe the gas of bosons by a non-relativistic 3 + 1-dimensional field theory. Being interested in static quantities at finite temperature, one works in the imaginary-time formalism in the grand canonical ensemble. The corresponding Euclidean action is

$$S_{3+1} = \int_0^\beta d\tau \int d^3x \left[ \psi^* \left( \frac{\partial}{\partial \tau} - \frac{1}{2m} \nabla^2 - \mu + V(\mathbf{x}) \right) \psi + \frac{2\pi a}{m} (\psi^* \psi)^2 \right], \quad (7)$$

with  $V(\mathbf{x}) = 0$  for the homogenous case and  $V(\mathbf{x}) = \frac{1}{2}m(\omega_x^2 x^2 + \omega_y^2 y^2 + \omega_z^2 z^2)$  for the harmonic trap. The complex field  $\psi$  is periodic in the imaginary-time direction,  $\psi(\mathbf{x}, 0) = \psi(\mathbf{x}, \beta)$ . The two-body interaction potential is parameterized by the  $s$ -wave scattering length  $a$ . It has been argued [7, 8] that the effect of interactions between more than two bosons and details of the two-body interaction potential beyond the  $s$ -wave scattering length enter only at higher orders in  $n^{1/3}$  and  $\lambda_0^{-1}$  than explicitly given in (2) and (6).

The effect of a wide trapping potential can be accommodated by writing

$$N_b = \int d^3x n(T, \mu - V(\mathbf{x})), \quad (8)$$

where the density function  $n(T, \mu)$  holds for the homogenous gas and, through the order needed here, may be obtained from a perturbative calculation [7, 9]. The relation (8) allows one to restrict all further field-theoretic considerations to the homogenous case [7].

Due to the imaginary-time periodicity of the field  $\psi(\mathbf{x}, \tau)$ , it may be decomposed into imaginary-time frequency modes with Matsubara frequencies  $\omega_j = 2\pi j/\beta$ . Subsequently, the nonzero Matsubara frequencies are integrated out, leaving a three-dimensional field theory for the zero-Matsubara modes  $\psi_0$ . Conventionally, this theory is written as

$$S_3 = \int d^3x \left[ \frac{1}{2} (\nabla \phi_a)^2 + \frac{r_B}{2} \phi_a^2 + \frac{u}{24} (\phi_a^2)^2 + f_B \right], \quad (9)$$

where  $\phi_a$  are  $N$  real field components, i.e.,  $a = 1, \dots, N$  and  $N = 2$  is the case interesting for BEC. In general,  $S_3$  contains a hierarchy of infinitely many terms, but for the orders given in (2) and (6), it is sufficient to consider the terms in (9). The relations between the parameters and fields in  $S_{3+1}$  and those of the effective field theory given by  $S_3$  may be determined by a perturbative matching calculation and are provided in [7, 8] through the order needed for the purposes here.

Finally, the coefficients in (2) are given by [8]

$$\bar{c}_1 = -\frac{4(4\pi)^3}{\zeta(\frac{3}{2})^{4/3}} \kappa_2, \quad (10a)$$

$$\check{c}'_2 = -\frac{16(4\pi)\zeta(\frac{1}{2})}{3\zeta(\frac{3}{2})^{5/3}} \approx 19.7518, \quad (10b)$$

$$\check{c}''_2 = \frac{16(4\pi)\zeta(\frac{1}{2})}{9\zeta(\frac{3}{2})^{5/3}} \ln[\zeta(\frac{3}{2})] + \frac{28(4\pi)^6}{\zeta(\frac{3}{2})^{8/3}} \kappa_2^2 + \frac{8(4\pi)}{3\zeta(\frac{3}{2})^{5/3}} \left\{ \frac{\zeta(\frac{1}{2})^2 \ln 2}{\sqrt{\pi}} + 2K_2 - \sqrt{\pi} - [\ln 2 + 3 \ln(4\pi) + 1 - 36(4\pi)^2 R_2 - 24(4\pi)^2 \kappa_2] \zeta(\frac{1}{2}) \right\}, \quad (10c)$$

with perturbatively defined  $K_2$  given in Appendix A and non-perturbative quantities  $\kappa_2$  and  $R_2$ , to which we return below. The coefficients in (6), on the other hand, are given by [7]

$$\check{c}_1 = \frac{2}{3\zeta(3)} \left[ \sum_{i,j=1}^{\infty} \frac{1}{i^{3/2} j^{3/2} (i+j)^{1/2}} - 2\zeta(2)\zeta(\frac{3}{2}) \right] \approx -3.426032, \quad (11a)$$

$$\check{c}'_2 = -\frac{8(4\pi)\zeta(2)}{3\zeta(3)} \approx -45.8566, \quad (11b)$$

$$\check{c}''_2 = C_2 - \frac{4(4\pi)\zeta(2)}{3\zeta(3)} [1 - \ln 2 + 3 \ln(4\pi) - 4K_1 - 36(4\pi)^2 R_2], \quad (11c)$$

with perturbatively defined  $K_1$  and  $C_2$  given in Appendix A and the same  $\kappa_2$  and  $R_2$  as in Eqs. (10).

The quantities  $\kappa_2$  and  $R_2$  remain to be computed within the three-dimensional theory. Although they are well-defined, their generalization from two to  $N$  real field components is not unique. We exploit this to define them in such a way that both their  $N \rightarrow 0$  and  $N \rightarrow \infty$  limits exist.

Let  $\kappa_N$  be the critical limit of the interaction-induced shift  $\Delta\langle\phi^2\rangle/Nu$  and let  $R_N$  be the critical limit of  $r_{\overline{\text{MS}}}(u, r)/(N+2)u^2$ , where  $r_{\overline{\text{MS}}}(u, r)$  is the renormalized version of the bare quantity defined by  $r_B(u, r) = r + \Sigma(0, u, r_B(u, r))$  with the self-energy  $\Sigma(k, u, r_B)$ . Here, renormalization refers to using the modified minimal subtraction scheme ( $\overline{\text{MS}}$ ) after applying dimensional regularization (DR). For  $R_N$ , we still have to specify the renormalization scale, which will be done below in Sec. II. Both  $\kappa_N$  and  $R_N$  receive contributions from all length scales, which makes them non-universal critical quantities. This is particularly obvious for  $R_N$  because of its renormalization scale dependence. Application of such quantities to physical situations is restricted to cases where the short-distance physics described by the effective field theory is perturbative at a scale where the effective theory is still applicable [8].

Our motivation to generalize  $\kappa_2$  and  $R_2$  to  $N$  real field components derives not only from the possibility to compare to the  $N = 1, 4$  Monte Carlo (MC) data of Sun [10], but also because our results may be applicable to physical situations different from BEC. We remind the reader that  $N = 0, 1, 2, 3$  correspond to the universality classes of dilute polymer solutions, the Ising model, the  $XY$  model, and the Heisenberg model, respectively.

We like to comment on the use of the phrase “universal.” In the context of critical phenomena, quantities are considered “universal” if they are common to all members of a given universality class. They do not depend on the microscopic Hamiltonian used to compute them, as long as the model under consideration is in the correct universality class. Universal quantities are typically critical exponents and critical amplitude ratios. In the context of BEC, on the other hand, “universal” refers to quantities that depend only on the  $s$ -wave scattering length  $a$  of the two-body interaction potential and on no further details of the potential such as the effective range  $r_s$  or interaction terms involving more than two particles. Consequently, the quantities  $\kappa_N$  and  $R_N$  are non-universal from the critical phenomena viewpoint, but  $\bar{c}_1, \bar{c}'_2, \bar{c}_1, \bar{c}'_2$ , and  $\bar{c}_2$  are universal BEC coefficients.

The remainder of this work is structured as follows. In Sec. II, we give a more detailed definition of the non-perturbative quantities  $\kappa_N$  and  $R_N$  and write down their loop expansions. In Sec. III, we determine the large- $N$  limit  $R_\infty$ . In Sec. IV we define the perturbative series for  $R_N$  and provide perturbative coefficients for  $N = 0, 1, 2, 3, 4, \infty$  through seven loops. In Sec. V, we resum the perturbative series using Kleinert’s variational perturbation theory (VPT) and obtain seven-loop estimates of  $R_N$  for  $N = 0, 1, 2, 3, 4, \infty$ . Previous results for  $\kappa_N$  with  $N = 1, 2, 4$  are extended to  $N = 0, 3$ . The results for  $\kappa_2$  and  $R_2$  are translated into values for  $\bar{c}'_2$  and  $\bar{c}_2$ , while the translation of our VPT results for  $\kappa_2$  was already given in [11–13]. We close with a discussion of our findings in Sec. VI.

## II. DEFINITION OF $\kappa_N$ AND $R_N$

As in [11–13] we use a renormalization scheme where the bare parameter  $r_B$  is traded for the renormalized quantity  $r \equiv r_B - \Sigma(0)$  with the self-energy  $\Sigma(p)$ . Full and free propagator are then

$$G(p) = \frac{1}{p^2 + r - [\Sigma(p) - \Sigma(0)]}, \quad G_0(p) = \frac{1}{p^2 + r}, \quad (12)$$

respectively, and the critical limit is identified as  $r \rightarrow 0$ . This scheme renders finite all diagrams in the expansion (13) below and all but the first two diagrams in the expansion (15) further below. This is essential for numerical evaluations, since it allows to work without regulator for all but these two diagrams. The two divergent diagrams will be regulated by DR and the only remaining

divergent diagram renormalized by  $\overline{\text{MS}}$ . The corresponding Feynman rules are  $\delta_{ab}G_0(p)$  for internal lines and  $-u(\delta_{ab}\delta_{cd} + \delta_{ac}\delta_{bd} + \delta_{ad}\delta_{bc})/3$  for vertices, where indices run from 1 to  $N$ . The integration measure for the loop momenta is  $\int_p \equiv \mu^\epsilon \int d^D p / (2\pi)^D$  with  $D = 3 - \epsilon$  and the renormalization scale  $\mu$ , whose introduction keeps the dimension of physical quantities at their  $D = 3$  values even for  $D \neq 3$ . For convergent diagrams, we may set  $D = 3$  from the outset, of course.

$\kappa_N$ , relevant for the first-order shift of  $T_c$  of a homogeneous Bose gas and also needed as one of the ingredients for the shift in second order for both the homogeneous gas and the case of a wide trap, has been determined before. We define it by  $\kappa_N \equiv \lim_{u_r \rightarrow \infty} \kappa_N(u_r)$ , where

$$\begin{aligned} \kappa_N(u_r) &\equiv \frac{\Delta\langle\phi^2\rangle}{Nu} = \frac{1}{u} \int_p [G(p) - G_0(p)] \\ &= \frac{1}{Nu} \left[ \mathcal{R} \left( \text{diagram 1} \right) + \mathcal{R} \left( \text{diagram 2} \right) + \dots \right] \end{aligned} \quad (13)$$

with

$$u_r \equiv \frac{(N+2)u}{\sqrt{r}}, \quad (14)$$

and where the operator  $\mathcal{R}$  recursively removes all zero-momentum parts of any self-energy subdiagram and originates in the subtraction of  $\Sigma(0)$  from  $\Sigma(p)$  in (12) [11–13]. The cross in the diagrams is an insertion that merely separates two propagators. Power counting shows that  $\kappa_N(u_r)$  depends on  $u$  and  $r$  only through the combination in (14). The inclusion of  $N+2$  in the definition of  $u_r$  leaves the perturbative coefficients of  $\kappa_N(u_r)$  finite for both  $N = 0$  and  $N \rightarrow \infty$ , when  $\kappa_N(u_r)$  is expressed as a power series in  $u_r$ .

Since we have computed  $\kappa_N$  [14] for  $N = 1, 2, 4$  in the framework of VPT through seven loops before [12, 13], we merely quote in Table I our results and those other results that appear to be most reliable (for detailed arguments supporting this conclusion, see [12] and references therein), namely those from MC simulations [10, 15–17]. Our results for  $N = 0, 3$  are new, though.

The other non-perturbative quantity needed for the second-order contributions (10c) and (11c) is the shift of the chemical potential due to the interaction [7, 8]. Within the three-dimensional theory (9), this amounts to computing the  $r \rightarrow 0$  limit of

$$\begin{aligned} r_B(u, r) &= r + \Sigma(0, u, r_B(u, r)) \\ &= r + \mathcal{R} \left( \text{diagram 1} \right) + \mathcal{R} \left( \text{diagram 2} \right) + \mathcal{R} \left( \text{diagram 3} \right) + \mathcal{R} \left( \text{diagram 4} \right) \\ &\quad + \dots \end{aligned} \quad (15)$$

at zero external momentum. This quantity, however, is ultraviolet (UV) divergent. The theory (9) is superrenormalizable, and only the one-loop diagram and the two-loop “sunset” diagram in the expansion (15) are divergent.

TABLE I:  $\kappa_N$  for  $N = 1, 2, 4$  from MC simulations, for  $N = 0, 1, 2, 3, 4$  from VPT through seven loops, and exact for  $N \rightarrow \infty$ . For obtaining the  $N = 0$  result from VPT, we have set  $\omega = 0.805$  and  $\eta = 0.029$  and thus  $\omega' = 0.8817$ , while for  $N = 3$ , we have set  $\omega = 0.785$  and  $\eta = 0.037$  and thus  $\omega' = 0.800$  (see, e.g., [18]). For  $N = 1, 2, 4$ , the reader is referred to [12].

$N$	$\kappa_N$ from MC	$\kappa_N$ from VPT
0	—	$-(3.66 \pm 0.39) \times 10^{-4}$
1	$-(4.94 \pm 0.41) \times 10^{-4}$ [10]	$-(4.86 \pm 0.45) \times 10^{-4}$ [12]
2	$-(5.85 \pm 0.23) \times 10^{-4}$ [15] $-(5.99 \pm 0.09) \times 10^{-4}$ [17]	$-(5.75 \pm 0.49) \times 10^{-4}$ [12]
3	—	$-(6.46 \pm 0.48) \times 10^{-4}$
4	$-(7.23 \pm 0.45) \times 10^{-4}$ [10]	$-(6.99 \pm 0.48) \times 10^{-4}$ [12]
$\infty$	$-1/[6(4\pi)^2] \approx -1.05543 \times 10^{-3}$ [3]	

Following [7, 8, 10], we use DR in  $D = 3 - \epsilon$  dimensions together with  $\overline{\text{MS}}$  to renormalize  $r_B$ . When using other schemes, the definition of the perturbative quantities in (10c) and (11c) would have to be changed as well, leading to the same values of  $\tilde{c}_2''$  and  $\tilde{c}_2''$ . The one-loop diagram in (15) is finite in DR and consequently needs no subtraction. The only divergent diagram is then the two-loop ‘‘sunset’’ diagram, which is computed in Appendix B. Using the results derived there, we define the renormalized quantity  $r_{\overline{\text{MS}}}(u, r)$  by

$$r_B(u, r) = r_{\overline{\text{MS}}}(u, r) + \frac{(N+2)u^2}{36(4\pi)^2\epsilon}. \quad (16)$$

$r_{\overline{\text{MS}}}(u, r)$  then remains finite as  $\epsilon \rightarrow 0$ . We further define  $R_N = \lim_{u_r \rightarrow \infty} R_N(u_r)$ , where

$$R_N(u_r) \equiv \lim_{\epsilon \rightarrow 0} \left. \frac{r_{\overline{\text{MS}}}(u, r)}{(N+2)u^2} \right|_{\bar{\mu}=(N+2)u/12} \quad (17)$$

with  $u_r$  from (14), and where  $\bar{\mu}$  is the renormalization scale in the  $\overline{\text{MS}}$  scheme, see also Appendix B. The relation with the quantity  $R \equiv \lim_{\epsilon \rightarrow 0} r_{\overline{\text{MS}}}(u, 0)/u^2|_{\bar{\mu}=u/3}$  determined for  $N = 2$  in [17] and for  $N = 1, 4$  in [10] is

$$R_N = \frac{R}{N+2} + \frac{1}{18(4\pi)^2} \ln \frac{N+2}{4}, \quad (18)$$

so that, for the BEC case  $N = 2$ ,

$$R = 4R_2. \quad (19)$$

Our definition leads to finite values for both  $R_0$  and  $R_\infty$ . The exact value of the latter will be computed next.

### III. $1/N$ -EXPANSION FOR $\kappa_N$ AND $R_N$

Consider expansions of  $\kappa_N$  and  $R_N$  in powers of  $N^{-1}$ , where  $u$  is considered to be proportional to  $N^{-1}$ , so that

$u_r$  is of order  $N^0$ . For the purposes of this section, each diagram represents only its leading order part in powers of  $N$ .

Denote the leading order (LO), next-to-leading order (NLO), etc. contributions to  $\kappa_N$  in a  $1/N$ -expansion by  $\kappa_N^{(0)}$ ,  $\kappa_N^{(1)}$ , etc., respectively, where  $\kappa_N^{(k)} \propto N^{-k}$ . In LO, only one type of diagrams contributes and, in general dimension  $D = 3 - \epsilon$ , we have

$$\begin{aligned} \kappa_\infty &= \kappa_N^{(0)} \\ &= \frac{1}{Nu} \lim_{r \rightarrow 0} \left[ \mathcal{R} \left( \text{Sunset} \right) + \mathcal{R} \left( \text{Triangle} \right) + \mathcal{R} \left( \text{Square} \right) + \dots \right] \\ &= -\frac{\pi\epsilon\gamma_\epsilon\mu^{2\epsilon}}{3(1+\epsilon)\sin\left(\frac{2\pi\epsilon}{1+\epsilon}\right)} \left( \frac{N\gamma_\epsilon\mu^\epsilon u}{6} \right)^{-2\epsilon/(1+\epsilon)} \frac{S_D}{(2\pi)^D}, \end{aligned} \quad (20)$$

where  $S_D = 2\pi^{D/2}/\Gamma(D/2)$  is the surface of a unit sphere in  $D$  dimensions. See Appendix C for intermediate steps. Taking the limit  $\epsilon \rightarrow 0$ , we get the result

$$\kappa_N = -\frac{1}{6(4\pi)^2} + \mathcal{O}(N^{-1}) \quad (21)$$

of [3], determined also in [19]. We have rederived the intermediate result (20) of [3] in our conventions since it turns out to be useful also for computing the large- $N$  limit of  $R_N$ .

Now consider  $r_{\overline{\text{MS}}}(u, 0)$  as defined by (15) and (16). In its  $1/N$ -expansion, denote the LO, NLO, etc. contributions to  $r_{\overline{\text{MS}}}(u, 0)$  by  $r_{\overline{\text{MS}}}^{(0)}(u, 0)$ ,  $r_{\overline{\text{MS}}}^{(1)}(u, 0)$ , etc. The first two terms on the right hand side of (15) are the only contributions to  $r_{\overline{\text{MS}}}(u, r)$  that are of order  $N^0$ . Since, observing (B1), they both vanish in DR as  $r \rightarrow 0$ , we get  $r_{\overline{\text{MS}}}^{(k)}(u, 0) \propto N^{-k-1}$ , up to logarithmic corrections of  $r_{\overline{\text{MS}}}^{(0)}(u, 0)$  and  $r_{\overline{\text{MS}}}^{(1)}(u, 0)$ , due to the UV divergence of the sunset diagram.

In LO,  $r_{\overline{\text{MS}}}(u, 0)$  receives contributions from two classes of diagrams and the counterterm defined in (16). The first contribution is

$$\begin{aligned} r_{\overline{\text{MS}}}^{(0a)}(u, 0) &= \lim_{r \rightarrow 0} \left[ \mathcal{R} \left( \text{Bubble} \right) + \mathcal{R} \left( \text{Sunset} \right) \right. \\ &\quad \left. + \mathcal{R} \left( \text{Sunset} \right) + \dots \right] \\ &= -\frac{Nu^2}{6\epsilon} \kappa_N^{(0)}, \end{aligned} \quad (22)$$

with intermediate steps provided in Appendix C.

The computation of the second contribution is even more closely related to that of  $\kappa_N^{(0)}$ ,

$$\begin{aligned} r_{\overline{\text{MS}}}^{(0b)}(u, 0) &= \lim_{r \rightarrow 0} \left[ \mathcal{R} \left( \text{Sunset} \right) + \mathcal{R} \left( \text{Triangle} \right) + \mathcal{R} \left( \text{Square} \right) + \dots \right] \\ &= -\frac{Nu^2}{6} \kappa_N^{(0)}, \end{aligned} \quad (23)$$

TABLE II: Numbers of diagrams for  $R_N$  in low loop orders  $l$ .

$l$	1	2	3	4	5	6	7	8	9
$n_l$	1	1	2	5	16	62	265	1387	8038

and we arrive at

$$\begin{aligned} r_{\overline{\text{MS}}}^{(0a)}(u, 0) + r_{\overline{\text{MS}}}^{(0b)}(u, 0) &= -\frac{Nu^2}{6\epsilon}(1 + \epsilon)\kappa_N^{(0)} \\ &= \frac{\pi\mu^\epsilon u}{3 \sin\left(\frac{2\pi\epsilon}{1+\epsilon}\right)} \left(\frac{N\gamma_\epsilon\mu^\epsilon u}{6}\right)^{(1-\epsilon)/(1+\epsilon)} \frac{S_D}{(2\pi)^D}. \end{aligned} \quad (24)$$

Subtracting from this the counterterm in (16) and taking the limit  $\epsilon \rightarrow 0$ , we obtain

$$\begin{aligned} r_{\overline{\text{MS}}}(u, 0) &= \frac{Nu^2}{18(4\pi)^2} \left(-\ln\frac{Nu}{\bar{\mu}} + 1 + 4\ln 2 + \ln 3\right) \\ &\quad + \mathcal{O}(N^{-2} \ln N). \end{aligned} \quad (25)$$

Setting  $\bar{\mu} = (N + 2)u/12$ , we arrive at

$$R_N = \frac{1 + 2 \ln 2}{18(4\pi)^2} + \mathcal{O}(N^{-1}), \quad (26)$$

from which we obtain the exact large- $N$  limit

$$R_\infty = \frac{1 + 2 \ln 2}{18(4\pi)^2} \approx 8.39521 \times 10^{-4}. \quad (27)$$

#### IV. PERTURBATIVE SERIES FOR $R_N$

The perturbative series corresponding to the loop expansion (13) of  $\kappa_N(u_r)$  and its resummation with VPT was discussed before in [11–13]. Note, however, that the use of  $N + 2$  (instead of  $N$  as in [11–13]) in the definition (14) of  $u_r$  is crucial for defining a perturbative expansion for  $\kappa_0(u_r)$ .

Here we focus on the perturbative series corresponding to the loop expansion of  $R_N(u_r)$ , defined by (15)–(17). We have constructed the relevant diagrams through seven loops using the recursive methods of [20]. The numbers of diagrams in some low loop orders is listed in Table II and the diagrams are collected in Table VI. A convenient representation of each diagram for symbolic manipulations by computer code was defined in [21] and is listed in Table VII and explained in Appendix D. The corresponding weights and group factors can be found in Tables VIII and IX, respectively. The integrals corresponding to the diagrams were computed by Nickel and Murray and were used for the determination of critical exponents for  $N = 0, 1, 2, 3$  in [21]. They were communicated to us by Nickel and are listed in Table VIII.

Through six loops, the numerical results for the integrals corresponding to the relevant diagrams were published in [22], while the seven-loop results have, to the best of our knowledge, never been published (except for

the small fraction of diagrams needed for the computation of  $\kappa_N$  [12]). We therefore provide the numerical results for the diagrams through seven loops in Table VIII.

Any subtracted  $l$ -loop diagram  $\mathcal{R}D_n$  represents the product  $\mathcal{R}D_n = (-u)^l w_n g_n I_n$ , where  $w_n$  is the combinatorial weight of the diagram,  $g_n$  its group factor from the  $O(N)$  symmetry and  $I_n$  the value of the corresponding integral. The only divergent diagrams have one and two loops, respectively, and are treated in Sec. II and in Appendix B. In DR, the one-loop diagram is in fact convergent.

Consider the case of zero external momentum, which is all we need for  $R_N$ . Dimensional analysis reveals that any  $l$ -loop integral  $I_n$  convergent in DR is proportional to  $r^{1-l/2}$  for  $D = 3$ . Therefore,  $I_n$  for any  $l$ -loop diagram with  $l \neq 2$  may be obtained from the  $r$ -derivative of  $I_n$  provided in Table VIII by

$$I_n = \frac{r^{1-l/2}}{1-l/2} \left. \frac{\partial I_n}{\partial r} \right|_{r=1}. \quad (28)$$

We conclude that the contribution from any  $l$ -loop integral with  $l \neq 2$  to  $R_N(u_r)$  is proportional to  $u_r^{l-2}$ . Combining (15)–(17), (B1), and (B7), we obtain

$$R_N(u_r) = b'_2 \ln u_r + \sum_{l=0}^{\infty} b_l u_r^{l-2} \quad (29)$$

with

$$b_0 = N + 2, \quad (30a)$$

$$b_1 = \frac{N + 2}{6(4\pi)}, \quad (30b)$$

$$b_2 = \frac{1 - 4 \ln 6}{36(4\pi)^2}, \quad (30c)$$

$$b'_2 = \frac{1}{18(4\pi)^2}. \quad (30d)$$

The higher-order perturbative coefficients  $b_l$  with  $l > 2$  have to be computed from the data in Tables VIII and IX. They are listed in Table III through  $l = 7$  for  $N = 0, 1, 2, 3, 4, \infty$ .

Note that the coefficients  $b_0$  and  $b_1$  diverge as  $N \rightarrow \infty$ . Since they multiply negative powers of  $u_r$ , this is not a problem if we take the limit  $u_r \rightarrow \infty$  before letting  $N \rightarrow \infty$ . This means that the terms involving  $b_0$  and  $b_1$  have to be dropped when resumming the perturbative series for  $N \rightarrow \infty$ , see also the following section.

#### V. RESUMMATION AND RESULTS

The loop expansions of  $\kappa_N(u_r)$  and  $R_N(u_r)$  suffer from infrared divergences as  $r \rightarrow 0$ , i.e., as  $u_r \rightarrow \infty$ . This corresponds to the well-known fact that the description of long-distance physics by perturbation theory breaks down at second-order phase transitions.

TABLE III: Perturbative coefficients  $b_l$  of the expansion (29) from three through seven loops for  $N = 0, 1, 2, 3, 4, \infty$ . The lower-loop coefficients  $b_0, b_1, b_2$ , and  $b'_2$  are provided in analytical form in Eqs. (30).

	$N = 0$	$N = 1$	$N = 2$	$N = 3$	$N = 4$	$N \rightarrow \infty$
$b_3$	$-8.91161 \times 10^{-6}$	$-6.51591 \times 10^{-6}$	$-5.31807 \times 10^{-6}$	$-4.59936 \times 10^{-6}$	$-4.12022 \times 10^{-6}$	$-1.72453 \times 10^{-6}$
$b_4$	$1.49970 \times 10^{-7}$	$8.09764 \times 10^{-8}$	$5.42095 \times 10^{-8}$	$4.06228 \times 10^{-8}$	$3.25956 \times 10^{-8}$	$4.82748 \times 10^{-9}$
$b_5$	$-4.00122 \times 10^{-9}$	$-1.59256 \times 10^{-9}$	$-8.72249 \times 10^{-10}$	$-5.64780 \times 10^{-10}$	$-4.04786 \times 10^{-10}$	$-1.89600 \times 10^{-11}$
$b_6$	$1.35890 \times 10^{-10}$	$3.96903 \times 10^{-11}$	$1.77165 \times 10^{-11}$	$9.87917 \times 10^{-12}$	$6.30620 \times 10^{-12}$	$8.60806 \times 10^{-14}$
$b_7$	$-5.42433 \times 10^{-12}$	$-1.15654 \times 10^{-12}$	$-4.19012 \times 10^{-13}$	$-2.00553 \times 10^{-13}$	$-1.13703 \times 10^{-13}$	$-4.23973 \times 10^{-16}$

The resummation of  $\kappa_N(u_r)$  through seven loops has been carried out in [12, 13] for  $N = 1, 2, 4$ , giving the results reported in Table I. We have added results for  $N = 0$  and  $N = 3$ .

Here we carry out the corresponding resummation of  $R_N(u_r)$ , given by the expansion (29). There are two relevant changes as compared to the resummation of  $\kappa_N(u_r)$ . One is the appearance of a logarithm of  $u_r$ . This turns out not to be an obstacle and VPT can be carried out as before. The other is the appearance of negative powers of  $u_r$  with nonzero coefficients  $b_0$  and  $b_1$ . These terms vanish in the limit  $u_r \rightarrow \infty$  and therefore do not contribute to  $R_N$ . However, such terms influence resummation. For the computation of  $\kappa_N$ , it was argued in [11–13] that it is most natural to work with a scheme where such negative powers are absent, but the same scheme leads to the nonzero coefficients  $b_0$  and  $b_1$  in (29). Below, we will in fact employ the ambiguity of not including one or both of these negative-power terms in our resummation procedure to estimate the precision of our result. For large  $N$ , one should drop the coefficients  $b_0$  and  $b_1$ , since they are the only ones to grow linearly with  $N$  and therefore make the perturbative series unnatural and consequently resummation with VPT tends not to work well if they are included.

The interactions cause the phase transition to be second order with critical exponents of the O(2) universality class. The leading class of corrections of a physical quantity that remains finite in the critical limit are integer powers of  $t^{\omega\nu}$  [18, 23, 24], where  $t \equiv (T - T_c)/T_c$ ,  $\nu$  is the critical exponent of the correlation length, and  $\omega = \beta'(g^*)$  in a renormalization group approach. Since, in our renormalization scheme, the propagator obeys  $G(p = 0) = 1/r \propto t^{-\gamma}$ , the leading corrections are integer powers of  $u_r^{-\omega'}$  with

$$\omega' = \frac{2\omega}{2 - \eta}. \quad (31)$$

Here we have employed the universal scaling relation  $\gamma = \nu(2 - \eta)$ , where  $\eta$  is the anomalous dimension of the critical propagator, i.e.,  $G(r = 0) \propto 1/p^{2-\eta}$  in the small- $p$  limit. If we neglect any other powers, we have

$$R_N(u_r) = \sum_{m=0}^{\infty} f_m u_r^{-m\omega'}. \quad (32)$$

Thus an expansion which correctly describes the leading corrections to scaling [23] has the form (32) with  $\omega'$  from (31).

The ansatz (32) does not account for so-called confluent singularities which cause the true large- $u_r$  expansion to also contain other negative powers of  $u_r$ , which are subleading at least compared to  $u_r^{-\omega'}$ . We can expect methods that can correctly accommodate the leading behavior in (32) to converge faster to the true result than methods having the wrong leading behavior, such as, e.g., Padé approximants or the linear delta expansion (LDE; see [25] for a general criticism of the application of the LDE in the context of field theory). On the other hand, convergence will be slowed by the fact that we do not make an ansatz reflecting the full power structure in  $u_r$ , but the expansion (32) will try to mimic the neglected subleading powers.

The alternating signs of the  $b_l$  displayed in Table III suggest that the perturbative series for  $R_N(u_r)$  is Borel summable. In the context of critical phenomena, such series have been successfully resummed using Kleinert's VPT (see [26–28] and Chapters 5 and 19 of the textbooks [29] and [18], respectively; improving perturbation theory by a variational principle goes back at least to [30]). Accurate critical exponents [18, 27, 28] and amplitude ratios [31] have been obtained. For a truncated partial sum through  $u_r^{L-2}$  of (29), the method requires replacing

$$u_r \rightarrow t\hat{u} \left\{ 1 + t \left[ \left( \frac{\hat{u}}{u_r} \right)^{\omega'} - 1 \right] \right\}^{-1/\omega'} \quad (33)$$

(note that this is an identity for  $t = 1$ ), reexpanding the resulting expression in  $t$  through  $t^{L-2}$ , setting  $t = 1$ , and then optimizing in  $\hat{u}$ , where optimizing is done in accordance with the principle of minimal sensitivity (PMS) [32] and in practice means finding appropriate stationary or turning points. While to the best of our knowledge, this has so far been done only for powers of  $u_r$ , the procedure goes straightforwardly through for the logarithmic term in (29) as well, if  $\ln t$  is treated as  $t^0$  for the purpose of power counting. Before optimizing, we may take the limit  $u_r \rightarrow \infty$ , since we are only interested in  $R_N = \lim_{u_r \rightarrow \infty} R_N(u_r)$ . The result is a function  $f_0^{(L)}(\hat{u}, \omega')$ , whose value optimized in  $\hat{u}$  is our  $L$ -loop VPT estimate  $f_0^{(L)}$  for  $f_0$  in the expansion (32), i.e., for  $R_N$ .

There are different ways of fixing the exponent  $\omega'$ . One may take it from other sources, since it is a universal critical exponent describing the approach to the critical point. One may selfconsistently determine it by setting to zero an appropriate logarithmic derivative of the quantity to be determined [18, 27]. These two approaches have been followed to determine  $\kappa_N$  in [11–13]. It turns out, however, that, for  $R_N$ , even when including up to seven-loop perturbative coefficients, these approaches do not lead to satisfactory plateaus when plotting  $f_0^{(L)}(\hat{u}, \omega')$  as a function of  $\hat{u}$ . However, the existence of such plateaus that become wider and flatter as the number of involved perturbative coefficients rises, is an indication that the PMS criterion works and therefore for the applicability of VPT to the problem at hand. We have therefore adopted an alternative approach [25], where  $\omega'$  is varied such that satisfactory plateaus develop. In practice, this means finding  $\omega'$  so that not only the first, but also the second or third derivative with respect to  $\hat{u}$  vanishes. As a check, it is mandatory to inspect the resulting plots of  $f_0^{(L)}(\hat{u}, \omega')$  as a function of  $\hat{u}$  for the resulting plateaus.

As mentioned above, the zero- and one-loop contributions to  $R_N(u_r)$  ultimately do not contribute to  $R_N$ . However, they influence resummation if only a finite number of perturbative coefficients are available. We have used the variance of the results when omitting the first or the first two orders in (29) to estimate the error of our estimates. The corresponding estimates for  $R_N$  as a function of the number of loops for  $N = 0, 1, 2, 3, 4, \infty$  can be found in Table IV. In Figs. 1,2,3, we plot these results for  $N = 1, 2, 4$  as a function of the number of loops together with the corresponding MC data.

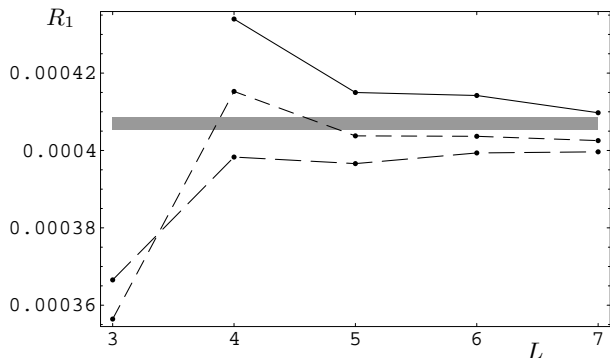


FIG. 1:  $R_1$  from VPT as a function of the number of loops  $L$ . Perturbative coefficients starting at zero loops (long dashes), one loop (short dashes) and two loops (solid) are used. The horizontal bar is the MC result including its error bar from Table V.

We conservatively estimate our mean result at the seven loop level by taking the average of the most distant of the three estimates and take their difference as the total error bar. This results in the values given in Table V, showing agreement with the corresponding MC values. Our VPT results and the MC data may also be compared to the large- $N$  result (27). Note that only the differences

TABLE IV: Results from VPT for  $10^4 R_N$  for  $N = 0, 1, 2, 3, 4, \infty$ . The perturbative coefficients involved are  $b_{l_{\min}}$  through  $b_{l_{\max}}$  in each case. Missing entries indicate that the PMS criterion does not provide a satisfactory solution or no solution at all. The data of this table for  $N = 1, 2, 4$  are, together with the corresponding MC data, visualized in Figs. 1,2,3, respectively.

$10^4 R_N$		$l_{\max}$				
$N$	$l_{\min}$	3	4	5	6	7
0	0	2.52263	3.23565	2.79559	2.83351	2.83130
	1	2.40522	3.02281	2.88227	2.88454	2.86700
	2		3.19514	2.98071	2.98519	2.93592
1	0	3.66540	3.98298	3.96602	3.99360	3.99648
	1	3.56421	4.15265	4.03773	4.03662	4.02549
	2		4.33980	4.14986	4.14212	4.09751
2	0		4.84689	4.74733	4.75283	4.75693
	1	4.32805	4.87315	4.78025	4.78056	4.77655
	2		5.07615	4.90577	4.89084	4.85027
3	0	5.15826	5.37860	5.28793	5.29284	5.29755
	1	4.88146	5.37527	5.30106	5.30329	5.30637
	2		5.59508	5.44013	5.42087	5.38362
4	0		5.75103	5.68154	5.68540	5.68979
	1	5.30578	5.74407	5.68587	5.68850	5.69231
	2		5.98154	5.83879	5.81683	5.78226
$\infty$	2		8.35299	8.39432	8.40716	8.40705

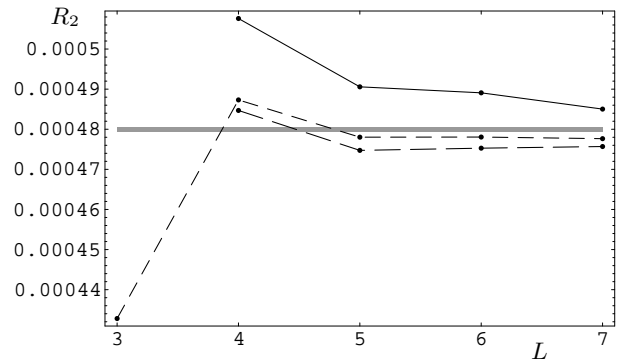
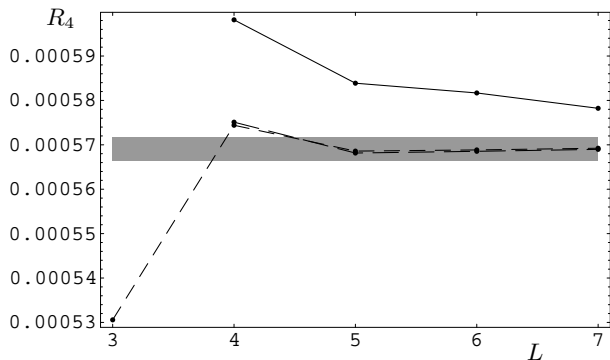


FIG. 2: Same as in Fig. 1, but for  $R_2$ .

between these values are relevant. This is due to the arbitrariness in fixing the scale  $\bar{\mu}$  that effectively separates perturbative from non-perturbative physics and causes a common arbitrary additive constant to the  $R_N$ .

We have also applied VPT to the large- $N$  case. As argued at the end of Sec. IV, we have to drop the one- and two-loop terms since  $b_0$  and  $b_1$  diverge as  $N \rightarrow \infty$ . In Fig. 4, we plot the results using fixed  $\omega' = 1$  (since  $\omega = 1$  and  $\eta = 0$  in this limit, see, e.g., [18]) and for the method of tuning  $\omega'$  as described above. The second method has faster apparent convergence than the one with  $\omega' = 1$ . However, it approaches the limiting value monotonously only for  $L \geq 6$ . This shows the potential

FIG. 3: Same as in Fig. 1, but for  $R_4$ .TABLE V:  $R_N$  for  $N = 1, 2, 4$  from MC simulations, for  $N = 0, 1, 2, 3, 4$  from VPT through seven loops, and exact for  $N \rightarrow \infty$ .

$N$	$R_N$ from MC	$R_N$ from VPT
0	—	$(2.884 \pm 0.052) \times 10^{-4}$
1	$(4.071 \pm 0.016) \times 10^{-4}$ [10]	$(4.047 \pm 0.051) \times 10^{-4}$
2	$(4.8003 \pm 0.0053) \times 10^{-4}$ [17]	$(4.804 \pm 0.047) \times 10^{-4}$
3	—	$(5.341 \pm 0.043) \times 10^{-4}$
4	$(5.690 \pm 0.027) \times 10^{-4}$ [10]	$(5.736 \pm 0.046) \times 10^{-4}$
$\infty$	$(1 + 2 \ln 2) / [18(4\pi)^2] \approx 8.39521 \times 10^{-4}$	

danger of making any extrapolations towards higher loop orders based on the VPT results through seven loops for the perturbative results for  $N < \infty$ .

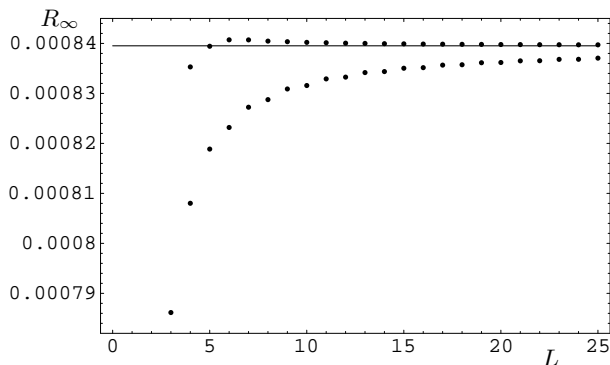


FIG. 4: Exact result for  $R_\infty$  (solid line) and perturbative results resummed with VPT as a function of the number of loops  $L$ . Lower dots: fixed  $\omega' = 1$ . Upper dots:  $\omega'$  from the plateau method, described in the main text. For  $N \rightarrow \infty$ , the perturbative coefficients  $b_l$  are easy to numerically compute at any loop order. Through seven loops, they are listed in Table III, while the corresponding VPT resummed values for  $R_\infty$  can be found in Table IV.

Using (10c) and (11c), our VPT results for  $\kappa_2$  given in

Table I and for  $R_2$  given in Table V translate into

$$\bar{c}_2'' = 74.6 \pm 2.3, \quad (34a)$$

$$\bar{c}_2'' = -155.0 \pm 0.7, \quad (34b)$$

which should be compared to the MC results [7, 8]

$$\bar{c}_2'' = 75.7 \pm 0.4, \quad (35a)$$

$$\bar{c}_2'' = -155.0 \pm 0.1, \quad (35b)$$

following from the MC data for  $\kappa_2$  and  $R_2$  given in Tables I and V, respectively.

Recently, an earlier attempt [33] to compute  $\bar{c}_2''$  using the LDE has been improved by using a generalization of the LDE that involves more free parameters [34]. These seem, however, to be introduced in a somewhat ad hoc manner, which makes it difficult to assess the validity of the method. Also, there is a small disagreement between our perturbative coefficients and those used there [35]. The results at five-loop order, the highest order considered for  $\bar{c}_2''$  in [34], lie between 73.5 and 79.3 and are therefore in good agreement with the MC data and our VPT results.

## VI. SUMMARY

We have applied VPT through seven loops to the computation of two non-perturbative non-universal quantities  $\kappa_N$  and  $R_N$  of critical  $O(N)$  symmetric  $\phi^4$  theory for  $N = 0, 1, 2, 3, 4$ . The results for  $\kappa_N$  and  $R_N$  are listed in Tables I and V, respectively. While for  $\kappa_N$  this was just an extension of earlier work [11–13] to  $N = 0, 3$ , the computation of  $R_N$  with VPT is new. Our results are in agreement with the apparently most reliable other results available obtained by MC simulations [10, 17]. For comparison, the MC results are also listed in Tables I and V. They are available only for  $N = 1, 2, 4$ , though.

In Tables VIII and IX, we provide all perturbative input data that allow for an extension of our results to other  $N$ , for checks of the input data and for other uses of these data. E.g., they have been used before to compute critical exponents for  $N = 0, 1, 2, 3$  [21]. The data, provided to us by Nickel, have, to the best of our knowledge, not previously been published.

In a computation similar to the one that lead to the large- $N$  limit  $\kappa_\infty$  [3], we have computed the exact large- $N$  limit  $R_\infty$ . The result is given in (27).

Employing the findings of [7, 8], our values  $\kappa_2$  and  $R_2$  may be translated into the coefficients  $\bar{c}_2''$  and  $\bar{c}_2''$  of the second-order shifts (2) and (6) of the BEC temperature for dilute homogenous and trapped Bose gases, respectively. This leads to the values in (34), which are in good agreement with the presumably most reliable other results (35) [7, 8], which follow from the MC data of [17] listed in Tables I and V.



### Acknowledgments

The author wishes to express his deep gratitude to B. Nickel for providing the results of his seven-loop calculations, without which this work would not have been possible. He thanks H. Kleinert for discussions and him as well as J.O. Andersen and B. Tomášik for a careful reading of the manuscript.

### APPENDIX A: PERTURBATIVE QUANTITIES CONTRIBUTING TO $\check{c}'_2$ AND $\check{c}''_2$

The perturbative constants needed in (10c) and (11c) are given by [8]

$$K_1 = \frac{1}{4\pi} \int_0^1 \frac{dt}{t} \left[ \text{Li}_{1/2}(t)^2 - \frac{\pi t}{1-t} \right] \approx -0.6305682, \quad (\text{A1})$$

$$K_2 = \frac{1}{4\pi} \int_0^1 \frac{ds}{s} \int_0^1 \frac{dt}{t} \left\{ \text{Li}_{1/2}(s)\text{Li}_{1/2}(t)\text{Li}_{-1/2}(st) - \frac{\sqrt{\pi}}{2} st(1-st)^{-3/2} \left[ \sqrt{\frac{\pi}{1-s}} + \zeta\left(\frac{1}{2}\right) \right] \left[ \sqrt{\frac{\pi}{1-t}} + \zeta\left(\frac{1}{2}\right) \right] \right\} \\ \approx -0.135083, \quad (\text{A2})$$

and [7]

$$C_2 = \frac{5}{2}\check{c}_1^2 + \frac{4}{3\zeta(3)} \left[ \zeta\left(\frac{3}{2}\right)^2 + 2\zeta\left(\frac{3}{2}\right) \sum_{i,j=1}^{\infty} \frac{(i+j)^{1/2} - i^{1/2} - j^{1/2}}{i^{3/2}j^{3/2}} \right. \\ \left. - 2 \sum_{i,j,k=1}^{\infty} \frac{1}{(ij)^{3/2}k^{1/2}} \left( \frac{1}{(i+j+k)^{1/2}} + \frac{ij}{(i+k)(j+k)(i+j+k)^{1/2}} - \frac{1}{k^{1/2}} \right) \right] \\ \approx 21.4 \quad (\text{A3})$$

with  $\check{c}_1$  from (11a).

### APPENDIX B: PERTURBATIVE ONE- AND TWO-LOOP DIAGRAMS

Here we compute the first two diagrams in (15). The one-loop diagram in (15), called 2-M1 in Table VI, is finite in DR for  $D \rightarrow 3$ . With the integration measure  $\int_p \equiv \mu^\epsilon \int d^D p / (2\pi)^D$  with  $D = 3 - \epsilon$ , it is given by

$$\mathcal{R} \text{ (diagram)} = \text{ (diagram)} = \frac{N+2}{6} (-u) \int_p \frac{1}{p^2+r} \\ = -\frac{N+2}{6} \frac{\mu^\epsilon u \Gamma\left(\frac{\epsilon}{2} - \frac{1}{2}\right)}{(4\pi)^{(3-\epsilon)/2} r^{\epsilon/2-1/2}} \\ = \frac{(N+2)u\sqrt{r}}{6(4\pi)} + \mathcal{O}(\epsilon). \quad (\text{B1})$$

The second, ‘‘sunset,’’ diagram in (15), called 3-S2 in Table VI, is the only diagram we need that is UV divergent in DR for  $D \rightarrow 3$ . At zero external momentum it is

given by

$$\mathcal{R} \text{ (diagram)} = \text{ (diagram)} \\ = \frac{N+2}{18} (-u)^2 \int_{pq} \frac{1}{(p^2+r)(q^2+r)[(p+q)^2+r]} \\ = \frac{(N+2)u^2}{18} (I_{2-1}^a + I_{2-1}^b), \quad (\text{B2})$$

where

$$I_{2-1}^a = \int_{pq} \frac{1}{p^2(q^2+r)[(p+q)^2+r]} \quad (\text{B3})$$

is divergent as  $D \rightarrow 3$  and will be computed in DR, and

$$I_{2-1}^b = -r \int_{pq} \frac{1}{p^2(p^2+r)(q^2+r)[(p+q)^2+r]} \quad (\text{B4})$$

is convergent for  $D = 3$ . For the computation of both  $I_{2-1}^a$  and  $I_{2-1}^b$  it is useful to introduce Feynman parameters.  $I_{2-1}^a$  can easily be computed in closed form in arbitrary dimension,

$$I_{2-1}^a = -\frac{1}{(4\pi)^3} \left( \frac{r}{4\pi\mu^2} \right)^{-\epsilon} \frac{\Gamma\left(\frac{\epsilon+1}{2}\right)\Gamma\left(\frac{\epsilon-1}{2}\right)}{\epsilon} \\ = \frac{1}{2(4\pi)^2} \left[ \frac{1}{\epsilon} - \ln \frac{r}{\mu^2} - 2 \ln 2 + 1 + \mathcal{O}(\epsilon) \right], \quad (\text{B5})$$

where  $\bar{\mu}$  is defined by  $4\pi\mu^2 = e^{\gamma_E}\bar{\mu}^2$  and the use of  $\bar{\mu}$  instead of  $\mu$  amounts by definition to working in  $\overline{\text{MS}}$  instead of minimal subtraction (MS).  $I_{2-1}^b$  is evaluated for  $D = 3$  with the result

$$I_{2-1}^b = -\frac{r}{(2\pi)^3} \int_0^\infty dp \frac{\arctan \frac{p}{2\sqrt{r}}}{p(p^2+r)} = \frac{1}{(4\pi)^2} \ln \frac{2}{3}. \quad (\text{B6})$$

Adding (B5) and (B6), we get

$$\mathcal{R} \text{---} \bigcirc = \frac{(N+2)u^2}{36(4\pi)^2} \left[ \frac{1}{\epsilon} - \ln \frac{r}{\bar{\mu}^2} - 2 \ln 3 + 1 + \mathcal{O}(\epsilon) \right]. \quad (\text{B7})$$

### APPENDIX C: LARGE- $N$ EXPANSION

Here we fill in the intermediate steps in deriving the results (20) and (22). The diagrams in (20) represent a geometric series, such that

$$\begin{aligned} \kappa_N^{(0)} &= \frac{Nu}{18} \int_k \left[ \Delta'(k) - \frac{1}{k^2} \int_p \frac{1}{p^4} \right] \frac{\Delta(k)}{1 + \frac{Nu}{6} \Delta(k)} \\ &= \frac{1}{3} \int_k \frac{\Delta'(k)}{1 + \left[ \frac{Nu}{6} \Delta(k) \right]^{-1}}, \end{aligned} \quad (\text{C1})$$

where

$$\Delta(k) \equiv \int_p \frac{1}{(k+p)^2 p^2} = \frac{\gamma_\epsilon \mu^\epsilon}{k^{1+\epsilon}} \quad (\text{C2})$$

and

$$\Delta'(k) \equiv \int_p \frac{1}{(k+p)^2 p^4} = \frac{\epsilon \gamma_\epsilon \mu^\epsilon}{k^{3+\epsilon}} \quad (\text{C3})$$

with

$$\gamma_\epsilon = \frac{\Gamma(\frac{1}{2} - \frac{\epsilon}{2})^2 \Gamma(\frac{1}{2} + \frac{\epsilon}{2})}{(4\pi)^{(3-\epsilon)/2} \Gamma(1-\epsilon)}, \quad (\text{C4})$$

as can easily be shown, e.g. using Feynman parameters. In (C1) we have used that the second term in the square brackets does not contribute, since in DR the integral over an arbitrary power  $s$  of  $p$  vanishes,

$$\int_p p^s = 0. \quad (\text{C5})$$

Changing the integration variable according to

$$k \rightarrow \left( \frac{N\gamma_\epsilon \mu^\epsilon u}{6} \right)^{1/(1+\epsilon)} k \quad (\text{C6})$$

gives

$$\kappa_N^{(0)} = \frac{\epsilon \gamma_\epsilon \mu^\epsilon}{3} \left( \frac{N\gamma_\epsilon \mu^\epsilon u}{6} \right)^{-2\epsilon/(1+\epsilon)} \int_k \frac{1}{k^{3+\epsilon}(1+k^{1+\epsilon})}. \quad (\text{C7})$$

Together with the identity

$$\int_0^\infty dk \frac{k^a}{1+k^b} = \frac{\pi}{b \sin \frac{(1+a)\pi}{b}}, \quad (\text{C8})$$

this leads immediately to the result (20).

The diagrams in (22) also represent a geometric series, such that

$$\begin{aligned} r_{\overline{\text{MS}}}^{(0a)}(u, 0) &= \frac{N(-u)^2}{18} \int_k \frac{\Delta(k)}{k^2 \left[ 1 + \frac{Nu}{6} \Delta(k) \right]} \\ &= \frac{u}{3} \int_k \frac{1}{k^2 \left\{ 1 + \left[ \frac{Nu}{6} \Delta(k) \right]^{-1} \right\}} \\ &= \frac{u}{3} \left( \frac{N\gamma_\epsilon \mu^\epsilon u}{6} \right)^{(1-\epsilon)/(1+\epsilon)} \int_k \frac{1}{k^2(1+k^{1+\epsilon})}. \end{aligned} \quad (\text{C9})$$

In the last step, we have changed the integration variable according to (C6). Due to (C5), we have

$$\int_k \frac{1}{k^2(1+k^{1+\epsilon})} = - \int_k \frac{1}{k^{3+\epsilon}(1+k^{1+\epsilon})} \quad (\text{C10})$$

and therefore, comparison with (C7) leads to (22).

### APPENDIX D: SYMBOLIC REPRESENTATION OF DIAGRAMS

In Table VII, we provide the representation of diagrams as defined in [36]. While the pictorial representation of Table VI is best for inspection by the human eye, the representation given in Table VII is useful for the symbolic manipulation of diagrams by computer code. Here we explain the rules for this representation along the lines of [36].

Label the  $n$  vertices of a diagram by integers 0 through  $n-1$  and construct the sequence

$$\begin{aligned} &/\text{vertices connected to } 0/ \text{ vertices connected to } \\ &1 \text{ excluding } 0/ \text{ vertices connected to } 2 \text{ excluding } \\ &0, 1/ \dots / \text{vertices connected to } m \text{ excluding } \\ &0, 1, \dots, m-1/ \dots / \text{vertices connected to } n-1 \\ &\text{excluding } 0, 1, \dots, n-2/ \end{aligned} \quad (\text{D1})$$

External lines are regarded as terminating on a vertex labeled E and are included in (D1). By convention, any line connecting a vertex to itself is listed only once. To any allowed sequence (D1) corresponds only one diagram, but to make the sequence unique requires additional rules.

Since the diagrams in which we are interested here have only vertices with four legs, it turns out that the slashes may be omitted from (D1) and that the labels E may be replaced by zeros without compromising the uniqueness of the diagram. If  $n_{\text{max}}$  is the maximal number of vertices in any diagram to be considered, choose this as the radix of the integers labeling the vertices in every diagram. Assuming this has been done, we apply the following rules.

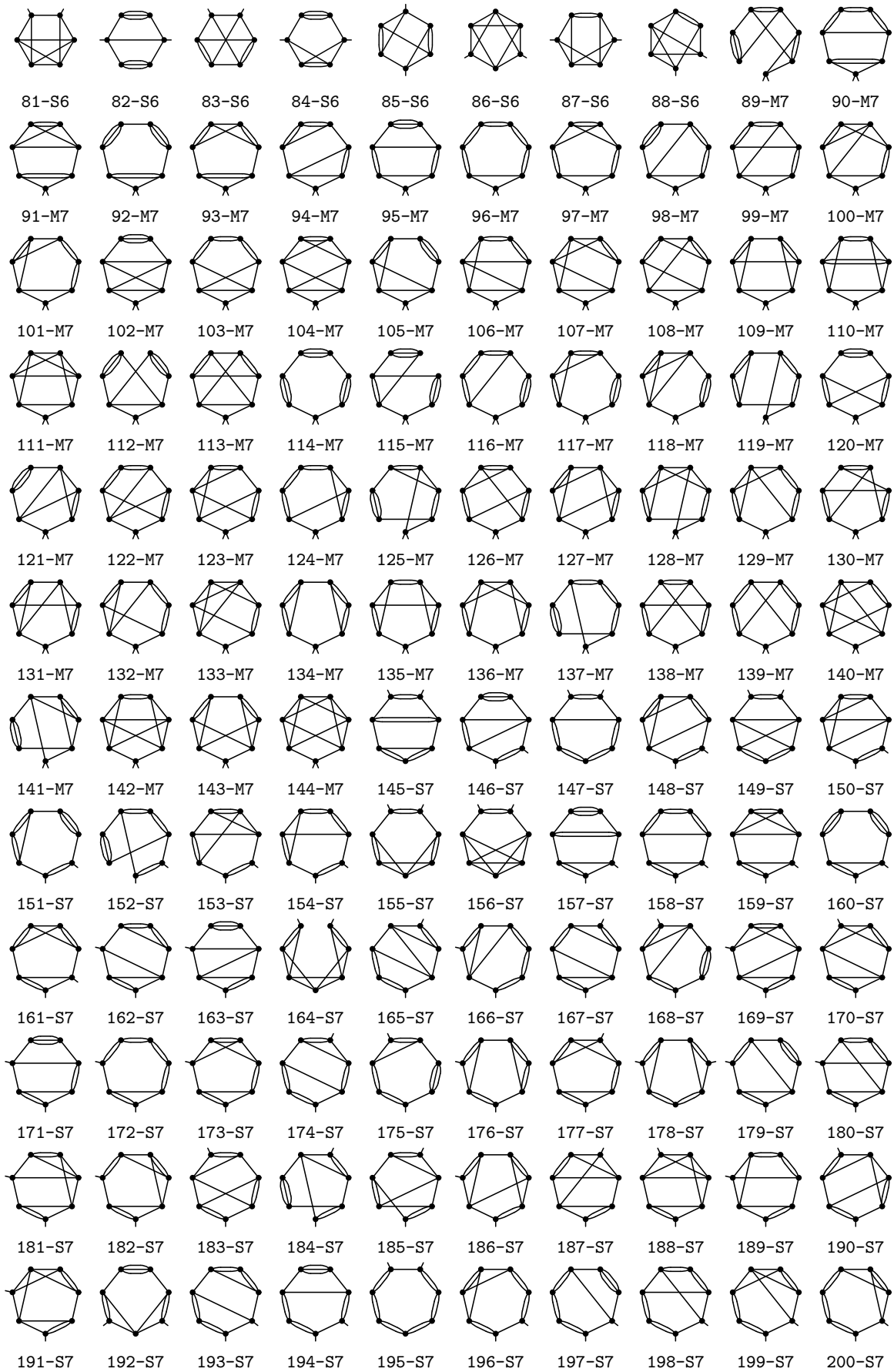
1. When listing from left to right the vertices connected to any one particular vertex, list E, if present, first and then the remaining integers in ascending order. Apply this rule to all vertices in turn; the resulting sequence is a unique description for the particular vertex labeling assigned to the diagram under consideration.
2. Form these unique sequences for all  $n!$  relabelings of the true vertices of the diagram.
3. Interpret each resulting sequence as a number and

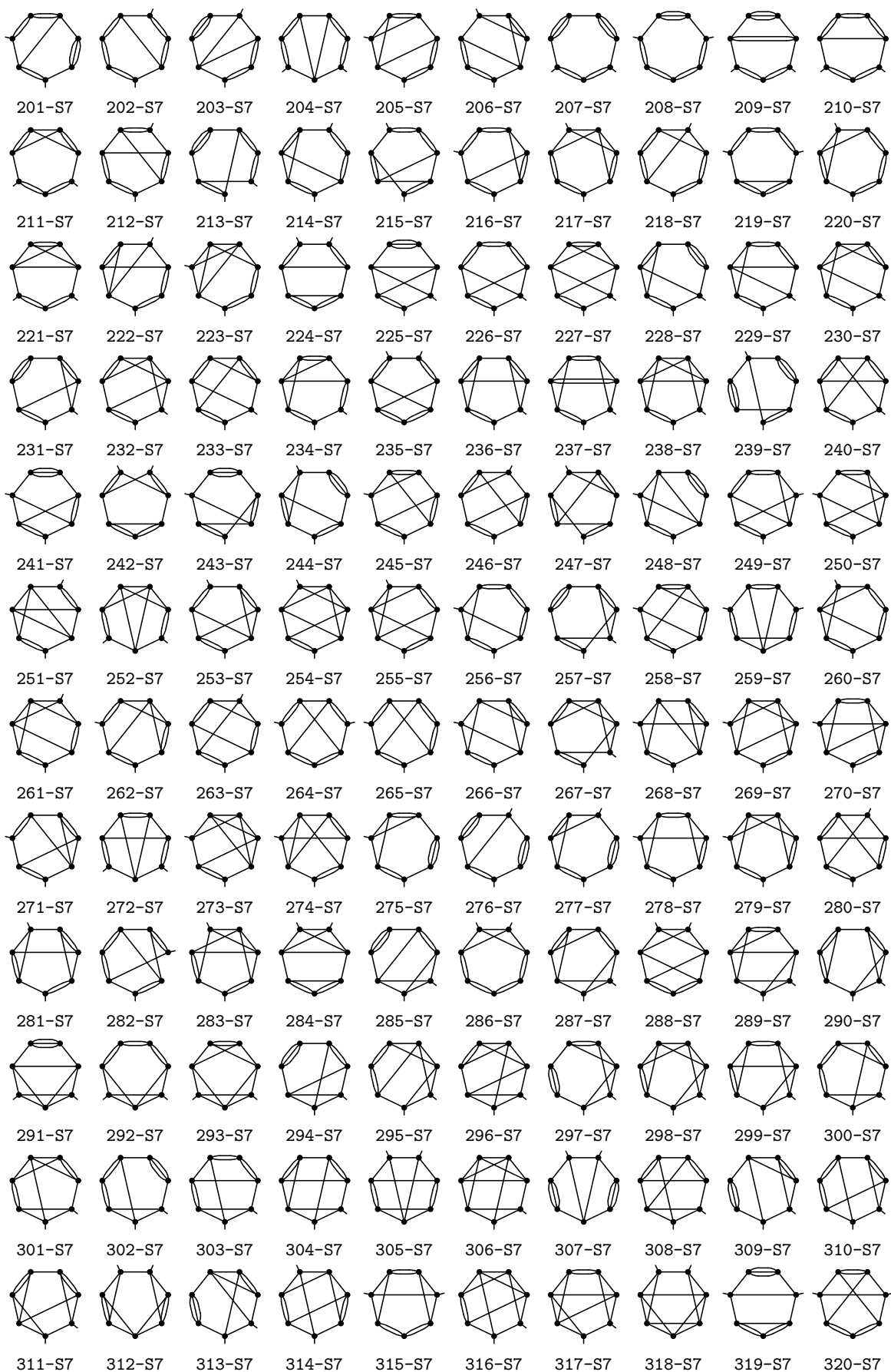
choose that sequence from step 2 that results in the smallest number as the unique descriptor for the diagram under consideration.

For better readability, the virtual vertex collecting the external lines may now be labeled by E again and the slashes may be reinstated, so that the format (D1) is recovered. As noted in [36], this is essentially the algorithm given by Nagle [37]. The diagrams in Tables VI, VII, and VIII are ordered by the numbers that result in step 3 above.

TABLE VI: Diagrams through seven loops A suitable representation for processing by computer code as defined in [36] may be found in Table VII. We do not provide a graphical representation of the zero-loop term  $k^2 + r$ , called 1-S0 in Table VII.

	2-M1	3-S2	4-M3	5-S3	6-M4	7-S4	8-S4	9-S4	10-S4
11-M5	12-M5	13-M5	14-M5	15-M5	16-S5	17-S5	18-S5	19-S5	20-S5
21-S5	22-S5	23-S5	24-S5	25-S5	26-S5	27-M6	28-M6	29-M6	30-M6
31-M6	32-M6	33-M6	34-M6	35-M6	36-M6	37-M6	38-M6	39-S6	40-S6
41-S6	42-S6	43-S6	44-S6	45-S6	46-S6	47-S6	48-S6	49-S6	50-S6
51-S6	52-S6	53-S6	54-S6	55-S6	56-S6	57-S6	58-S6	59-S6	60-S6
61-S6	62-S6	63-S6	64-S6	65-S6	66-S6	67-S6	68-S6	69-S6	70-S6
71-S6	72-S6	73-S6	74-S6	75-S6	76-S6	77-S6	78-S6	79-S6	80-S6





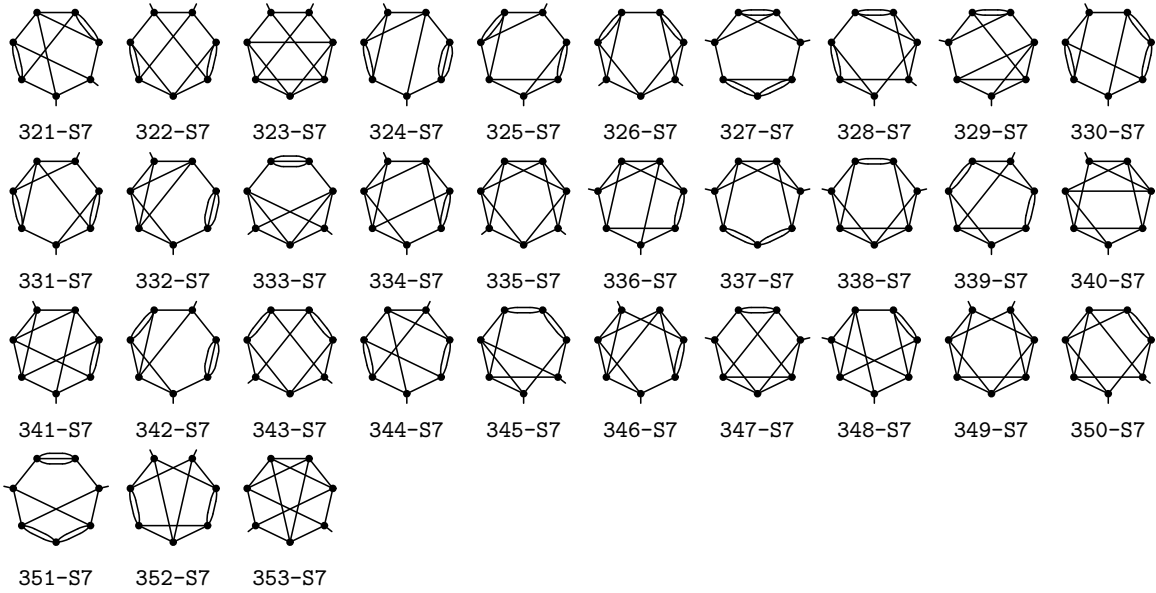


TABLE VII: Suitable representation of diagrams for processing by computer code according to [36]. Explanations are given in Appendix D.

diagram	code	diagram	code	diagram	code
1-S0	//	119-M7	/EE12/334/335/566/66//	237-S7	/E112/34/E56/455/66/6//
2-M1	/EE0/	120-M7	/EE12/334/344/5/6/666//	238-S7	/E112/34/E56/456/56/6//
3-S2	/E111/E/	121-M7	/EE12/334/345/4/6/666//	239-S7	/E112/34/E56/555/666//
4-M3	/EE12/222//	122-M7	/EE12/334/345/5/66/66//	240-S7	/E112/34/E56/556/566//
5-S3	/E112/22/E/	123-M7	/EE12/334/345/6/56/66//	241-S7	/E112/34/334/5/E6/666//
6-M4	/EE12/233/33//	124-M7	/EE12/334/355/4/66/66//	242-S7	/E112/34/335/E/566/66//
7-S4	/E112/E3/333//	125-M7	/EE12/334/355/5/666/6//	243-S7	/E112/34/335/4/E6/666//
8-S4	/E112/23/33/E/	126-M7	/EE12/334/355/6/566/6//	244-S7	/E112/34/335/5/666/E6//
9-S4	/E112/33/E33//	127-M7	/EE12/334/356/4/56/66//	245-S7	/E112/34/335/6/E56/66//
10-S4	/E123/E23/33//	128-M7	/EE12/334/356/5/566/6//	246-S7	/E112/34/335/6/556/6/E//
11-M5	/EE12/223/4/444//	129-M7	/EE12/334/356/5/666/6//	247-S7	/E112/34/335/6/666/E6//
12-M5	/EE12/233/44/44//	130-M7	/EE12/334/356/6/666/6//	248-S7	/E112/34/345/E4/6/666//
13-M5	/EE12/234/34/44//	131-M7	/EE12/334/356/6/666/6//	249-S7	/E112/34/345/E5/66/66//
14-M5	/EE12/333/444/4//	132-M7	/EE12/334/356/6/666/6//	250-S7	/E112/34/345/E6/56/66//
15-M5	/EE12/334/344/4//	133-M7	/EE12/334/356/6/666/6//	251-S7	/E112/34/345/E6/66/E//
16-S5	/E112/E3/344/44//	134-M7	/EE12/334/356/6/666/6//	252-S7	/E112/34/345/E6/66/E//
17-S5	/E112/23/E4/444//	135-M7	/EE12/334/356/6/666/6//	253-S7	/E112/34/345/E6/66/E//
18-S5	/E112/23/34/44/E//	136-M7	/EE12/334/356/6/666/6//	254-S7	/E112/34/345/E6/66/E//
19-S5	/E112/23/44/E44//	137-M7	/EE12/334/356/6/666/6//	255-S7	/E112/34/345/E6/66/E//
20-S5	/E112/33/E44/44//	138-M7	/EE12/334/356/6/666/6//	256-S7	/E112/34/345/E6/66/E//
21-S5	/E112/33/444/E4//	139-M7	/EE12/334/356/6/666/6//	257-S7	/E112/34/345/E6/66/E//
22-S5	/E112/34/E34/44//	140-M7	/EE12/345/346/46/6/66//	258-S7	/E112/34/345/E6/66/E//
23-S5	/E112/34/334/4/E//	141-M7	/EE12/345/346/46/6/66//	259-S7	/E112/34/345/E6/66/E//
24-S5	/E123/E23/44/44//	142-M7	/EE12/345/346/46/6/66//	260-S7	/E112/34/345/E6/66/E//
25-S5	/E123/E24/34/44//	143-M7	/EE12/345/346/46/6/66//	261-S7	/E112/34/345/E6/66/E//
26-S5	/E123/234/34/4/E//	144-M7	/EE12/345/346/46/6/66//	262-S7	/E112/34/345/E6/66/E//
27-M6	/EE12/223/4/455/55//	145-S7	/E112/E3/334/5/666/66//	263-S7	/E112/34/345/E6/66/E//
28-M6	/EE12/233/34/5/555//	146-S7	/E112/E3/334/5/666/66//	264-S7	/E112/34/345/E6/66/E//
29-M6	/EE12/233/44/55/55//	147-S7	/E112/E3/334/5/666/66//	265-S7	/E112/34/345/E6/66/E//
30-M6	/EE12/233/45/45/55//	148-S7	/E112/E3/334/5/666/66//	266-S7	/E112/34/345/E6/66/E//
31-M6	/EE12/234/34/55/55//	149-S7	/E112/E3/334/5/666/66//	267-S7	/E112/34/345/E6/66/E//
32-M6	/EE12/234/35/45/55//	150-S7	/E112/E3/334/5/666/66//	268-S7	/E112/34/345/E6/66/E//
33-M6	/EE12/333/445/5/55//	151-S7	/E112/E3/334/5/666/66//	269-S7	/E112/34/345/E6/66/E//
34-M6	/EE12/334/335/555//	152-S7	/E112/E3/334/5/666/66//	270-S7	/E112/34/345/E6/66/E//
35-M6	/EE12/334/345/5/55//	153-S7	/E112/E3/334/5/666/66//	271-S7	/E112/34/345/E6/66/E//
36-M6	/EE12/334/355/4/55//	154-S7	/E112/E3/334/5/666/66//	272-S7	/E112/34/345/E6/66/E//
37-M6	/EE12/334/455/45/5//	155-S7	/E112/E3/334/5/666/66//	273-S7	/E112/34/345/E6/66/E//
38-M6	/EE12/345/345/45/5//	156-S7	/E112/E3/334/5/666/66//	274-S7	/E112/34/345/E6/66/E//
39-S6	/E112/E3/334/5/555//	157-S7	/E112/23/E4/445/6/666//	275-S7	/E112/34/345/E6/66/E//
40-S6	/E112/E3/344/55/55//	158-S7	/E112/23/E4/445/6/666//	276-S7	/E112/34/345/E6/66/E//
41-S6	/E112/E3/345/45/55//	159-S7	/E112/23/E4/445/6/666//	277-S7	/E112/34/345/E6/66/E//
42-S6	/E112/E3/444/555/5//	160-S7	/E112/23/E4/445/6/666//	278-S7	/E112/34/345/E6/66/E//
43-S6	/E112/E3/445/455/5//	161-S7	/E112/23/E4/445/6/666//	279-S7	/E112/34/345/E6/66/E//

44-S6	/E112/23/E4/455/55//	162-S7	/E112/23/34/E5/566/66//	280-S7	/E112/34/556/E56/566//
45-S6	/E112/23/34/E5/555//	163-S7	/E112/23/34/45/E6/666//	281-S7	/E112/34/556/445/6/6/E/
46-S6	/E112/23/34/45/55/E/	164-S7	/E112/23/34/45/56/66/E/	282-S7	/E112/34/556/455/66/E/
47-S6	/E112/23/34/55/E55//	165-S7	/E112/23/34/45/66/E66//	283-S7	/E112/34/556/456/56/E/
48-S6	/E112/23/44/E55/55//	166-S7	/E112/23/34/55/E66/66//	284-S7	/E123/E23/34/5/566/66//
49-S6	/E112/23/44/455/5/E/	167-S7	/E112/23/34/55/566/6/E/	285-S7	/E123/E23/44/45/6/666//
50-S6	/E112/23/44/555/E5//	168-S7	/E112/23/34/55/666/E6//	286-S7	/E123/E23/44/55/66/66//
51-S6	/E112/23/45/E45/55//	169-S7	/E112/23/34/56/E56/66//	287-S7	/E123/E23/44/56/56/66//
52-S6	/E112/23/45/445/5/E/	170-S7	/E112/23/34/56/556/6/E/	288-S7	/E123/E23/45/46/66/66//
53-S6	/E112/33/E34/5/555//	171-S7	/E112/23/44/E45/6/666//	289-S7	/E123/E23/45/46/56/66//
54-S6	/E112/33/E44/55/55//	172-S7	/E112/23/44/E55/66/66//	290-S7	/E123/E24/33/5/566/66//
55-S6	/E112/33/E45/45/55//	173-S7	/E112/23/44/E56/56/66//	291-S7	/E123/E24/34/45/6/666//
56-S6	/E112/33/344/5/55/E/	174-S7	/E112/23/44/455/6/66/E/	292-S7	/E123/E24/34/55/66/66//
57-S6	/E112/33/444/55/5/E/	175-S7	/E112/23/44/555/66/6/E/	293-S7	/E123/E24/34/56/56/66//
58-S6	/E112/33/445/E5/55//	176-S7	/E112/23/44/556/E6/66//	294-S7	/E123/E24/35/44/6/666//
59-S6	/E112/33/445/45/5/E/	177-S7	/E112/23/44/556/56/6/E/	295-S7	/E123/E24/35/45/66/66//
60-S6	/E112/34/E33/5/555//	178-S7	/E112/23/44/556/66/E6//	296-S7	/E123/E24/35/46/56/66//
61-S6	/E112/34/E34/55/55//	179-S7	/E112/23/45/E44/6/666//	297-S7	/E123/E24/35/55/666/6//
62-S6	/E112/34/E35/45/55//	180-S7	/E112/23/45/E45/66/66//	298-S7	/E123/E24/35/56/566/6//
63-S6	/E112/34/E55/445/5//	181-S7	/E112/23/45/E46/56/66//	299-S7	/E123/E24/35/66/556/6//
64-S6	/E112/34/E34/34/5/55/E/	182-S7	/E112/23/45/E66/556/6//	300-S7	/E123/E24/55/446/6/66//
65-S6	/E112/34/335/E/555//	183-S7	/E112/23/45/445/6/66/E/	301-S7	/E123/E24/55/456/66/6//
66-S6	/E112/34/335/4/55/E/	184-S7	/E112/23/45/446/E/666//	302-S7	/E123/E24/55/556/666//
67-S6	/E112/34/335/5/E55//	185-S7	/E112/23/45/446/5/66/E/	303-S7	/E123/E24/55/566/566//
68-S6	/E112/34/345/E5/55//	186-S7	/E112/23/45/446/6/E66//	304-S7	/E123/E24/56/445/6/66//
69-S6	/E112/34/345/45/5/E/	187-S7	/E112/23/45/456/E6/66//	305-S7	/E123/E24/56/455/66/6//
70-S6	/E112/34/355/E4/55//	188-S7	/E112/23/45/456/56/6/E/	306-S7	/E123/E24/56/456/56/6//
71-S6	/E112/34/355/45/E5//	189-S7	/E112/23/45/466/E5/66//	307-S7	/E123/E24/56/555/666//
72-S6	/E123/E23/34/5/555//	190-S7	/E112/23/45/466/55/6/E/	308-S7	/E123/E24/56/556/566//
73-S6	/E123/E23/44/55/55//	191-S7	/E112/23/45/466/56/E6//	309-S7	/E123/E45/334/4/6/666//
74-S6	/E123/E23/45/45/55//	192-S7	/E112/23/45/666/E55/6//	310-S7	/E123/E45/334/5/66/66//
75-S6	/E123/E24/33/5/555//	193-S7	/E112/33/E34/5/566/66//	311-S7	/E123/E45/334/6/56/66//
76-S6	/E123/E24/34/55/55//	194-S7	/E112/33/E44/45/6/666//	312-S7	/E123/E45/336/6/556/6//
77-S6	/E123/E24/35/45/55//	195-S7	/E112/33/E44/55/66/66//	313-S7	/E123/E45/344/46/666//
78-S6	/E123/E24/55/445/5//	196-S7	/E112/33/E44/56/56/66//	314-S7	/E123/E45/344/56/6/66//
79-S6	/E123/E45/334/5/55//	197-S7	/E112/33/E45/44/6/666//	315-S7	/E123/E45/344/66/5/66//
80-S6	/E123/E45/344/55/5//	198-S7	/E112/33/E45/45/66/66//	316-S7	/E123/E45/345/46/6/66//
81-S6	/E123/E45/345/45/5//	199-S7	/E112/33/E45/46/56/66//	317-S7	/E123/E45/345/66/56/6//
82-S6	/E123/E45/444/555//	200-S7	/E112/33/E45/66/556/6//	318-S7	/E123/E45/346/56/56/6//
83-S6	/E123/E45/445/455//	201-S7	/E112/33/344/5/E6/666//	319-S7	/E123/E45/444/566/66//
84-S6	/E123/224/4/555/E5//	202-S7	/E112/33/344/5/66/E66//	320-S7	/E123/E45/445/466/66//
85-S6	/E123/224/5/445/5/E/	203-S7	/E112/33/345/4/E6/666//	321-S7	/E123/E45/445/566/6/6//
86-S6	/E123/234/45/45/5/E/	204-S7	/E112/33/345/4/66/E66//	322-S7	/E123/E45/446/556/6/6//
87-S6	/E123/234/45/55/E5//	205-S7	/E112/33/345/6/E56/66//	323-S7	/E123/E45/456/456/6/6//
88-S6	/E123/245/45/445/E/	206-S7	/E112/33/345/6/556/6/E/	324-S7	/E123/224/4/45/E6/666//
89-M7	/EE12/223/4/445/6/666//	207-S7	/E112/33/444/E5/6/666//	325-S7	/E123/223/4/56/E56/66//
90-M7	/EE12/223/4/455/66/66//	208-S7	/E112/33/444/55/6/66/E/	326-S7	/E123/223/4/56/556/6/E/
91-M7	/EE12/223/4/456/56/66//	209-S7	/E112/33/445/E4/6/666//	327-S7	/E123/224/4/556/E6/66//
92-M7	/EE12/223/4/555/666/6//	210-S7	/E112/33/445/E5/66/66//	328-S7	/E123/224/5/456/E6/66//
93-M7	/EE12/223/4/556/566/6//	211-S7	/E112/33/445/E6/56/66//	329-S7	/E123/224/5/456/56/6/E/
94-M7	/EE12/233/34/5/566/66//	212-S7	/E112/33/445/45/6/66/E/	330-S7	/E123/224/5/466/E5/66//
95-M7	/EE12/233/44/45/6/666//	213-S7	/E112/33/445/46/E/666//	331-S7	/E123/224/5/466/56/E6//
96-M7	/EE12/233/44/55/66/66//	214-S7	/E112/33/445/46/5/66/E/	332-S7	/E123/234/34/5/E6/666//
97-M7	/EE12/233/44/56/56/66//	215-S7	/E112/33/445/46/6/E66//	333-S7	/E123/234/45/46/E/666//
98-M7	/EE12/233/45/44/6/666//	216-S7	/E112/33/445/56/E6/66//	334-S7	/E123/234/45/56/E6/66//
99-M7	/EE12/233/45/45/66/66//	217-S7	/E112/33/445/56/56/6/E/	335-S7	/E123/234/45/56/56/6/E/
100-M7	/EE12/233/45/46/56/66//	218-S7	/E112/33/445/56/66/E6//	336-S7	/E123/234/45/56/66/E6//
101-M7	/EE12/233/45/66/556/6//	219-S7	/E112/33/445/66/55/6/E/	337-S7	/E123/234/45/66/E5/66//
102-M7	/EE12/234/34/45/6/666//	220-S7	/E112/33/445/66/56/E6//	338-S7	/E123/234/45/66/56/E6//
103-M7	/EE12/234/34/55/66/66//	221-S7	/E112/33/456/E4/56/66//	339-S7	/E123/234/55/66/E56/6//
104-M7	/EE12/234/34/56/56/66//	222-S7	/E112/33/456/45/E6/66//	340-S7	/E123/234/56/56/E56/6//
105-M7	/EE12/234/35/44/6/666//	223-S7	/E112/33/456/45/56/6/E/	341-S7	/E123/234/56/56/556/E/
106-M7	/EE12/234/35/45/66/66//	224-S7	/E112/34/E33/5/566/66//	342-S7	/E123/244/45/666/5/E6//
107-M7	/EE12/234/35/46/56/66//	225-S7	/E112/34/E34/45/6/666//	343-S7	/E123/244/56/455/6/6/E/
108-M7	/EE12/234/35/66/556/6//	226-S7	/E112/34/E34/55/66/66//	344-S7	/E123/244/56/556/56/E/
109-M7	/EE12/234/56/445/6/66//	227-S7	/E112/34/E34/56/56/66//	345-S7	/E123/245/45/466/E/66//
110-M7	/EE12/234/56/455/66/6//	228-S7	/E112/34/E35/44/6/666//	346-S7	/E123/245/45/466/6/E6//
111-M7	/EE12/234/56/456/56/6//	229-S7	/E112/34/E35/45/66/66//	347-S7	/E123/245/46/455/6/6/E/
112-M7	/EE12/234/56/555/666//	230-S7	/E112/34/E35/46/56/66//	348-S7	/E123/245/46/456/E/66//
113-M7	/EE12/234/56/556/566//	231-S7	/E112/34/E35/55/666/6//	349-S7	/E123/245/46/456/5/6/E/
114-M7	/EE12/333/444/5/6/666//	232-S7	/E112/34/E35/56/566/6//	350-S7	/E123/245/46/556/56/E/
115-M7	/EE12/333/445/4/6/666//	233-S7	/E112/34/E35/66/556/6//	351-S7	/E123/444/556/556/6/E/
116-M7	/EE12/333/445/5/66/66//	234-S7	/E112/34/E55/456/66/6//	352-S7	/E123/445/456/566/6/E/
117-M7	/EE12/333/445/6/56/66//	235-S7	/E112/34/E55/566/566//	353-S7	/E123/456/456/456/E/6//

TABLE VIII: Weights  $w_n$ , group factors  $g_n$  and numerical results for diagrams through seven loops (\* = probable error in the final digit; \*\* = probable error in the two final digits; () = estimated statistical error in final digits). The explicit group factors are listed in Table IX. The numerical data were provided by B. Nickel and have only partially been checked by the author. The numbering proceeds according to [36]. Since the momentum derivatives have not been published before, we also provide them here, although they are not needed for the purposes of this work. The numerical values are taken at  $r = 1$  and  $k = 0$ , and  $l$  is the number of loops of the corresponding diagram, indicated by the last digit of the diagram name  $n$ .

$n$	$w_n$	$g_n$	$-(8\pi)^l \frac{\partial I_n}{\partial r}$	$-(8\pi)^l \frac{\partial I_n}{\partial k^2}$	$n$	$w_n$	$g_n$	$-(8\pi)^l \frac{\partial I_n}{\partial r}$	$-(8\pi)^l \frac{\partial I_n}{\partial k^2}$
1-S0	1	1	-1.000000000000	-1.000000000000	178-S7	1/16	$g_{46}$	1.112198567717	0.059426697530
2-M1	1/2	$g_1$	1.000000000000	0	179-S7	1/12	$g_{15}$	-0.099385135580	-0.003196017365
3-S2	1/6	$g_1$	2.000000000000	0.074074074074	180-S7	1/8	$g_{47}$	0.613041462344	0.025955207773
4-M3	1/12	$g_2$	-0.575364144904	0	181-S7	1/2	$g_{44}$	0.477782071483	0.020153442432
5-S3	1/4	$g_3$	2.053735627745	0.094651431944	182-S7	1/8	$g_{46}$	0.822000194835	0.039293990833
6-M4	1/8	$g_4$	-0.817603121794	0	183-S7	1/4	$g_{41}$	0.62652529607	0.03117089736
7-S4	1/12	$g_5$	-0.296452722985	-0.003098338156	184-S7	1/12	$g_{16}$	-0.088398198119	-0.002799922292
8-S4	1/4	$g_2$	1.723490549736	0.086595023215	185-S7	1/4	$g_{48}$	0.633014398591	0.031431108546
9-S4	1/8	$g_6$	2.065719357141	0.101317290347	186-S7	1/4	$g_{44}$	0.69594974685	0.03412961347
10-S4	1/4	$g_5$	1.240596097829	0.050040931841	187-S7	1/2	$g_{41}$	0.44224379962	0.01909934773
11-M5	1/24	$g_7$	0.063289032026	0	188-S7	1/2	$g_{49}$	0.2738240559**	0.0117842659*
12-M5	1/16	$g_8$	-0.950830436253	0	189-S7	1/4	$g_{42}$	0.587039378427	0.025512006666
13-M5	1/8	$g_9$	-0.522389299127	0	190-S7	1/4	$g_{50}$	0.71485758848	0.03528193562
14-M5	1/72	$g_7$	0.034976834929	0	191-S7	1/2	$g_{41}$	0.45315198278	0.01965173249
15-M5	1/8	$g_9$	-0.810810317465	0	192-S7	1/24	$g_{16}$	-0.091382042321	-0.002633887708
16-S5	1/8	$g_4$	-0.432936983596	-0.003699002180	193-S7	1/8	$g_{40}$	-0.200696579093	-0.004500005469
17-S5	1/6	$g_4$	-0.184366712188	-0.003701938896	194-S7	1/24	$g_{14}$	-0.128843563571	-0.003942067525
18-S5	1/4	$g_{10}$	1.280344835327	0.067020792129	195-S7	1/64	$g_{51}$	2.024860402022	0.099350544942
19-S5	1/4	$g_{11}$	1.608449036612	0.083298877665	196-S7	1/16	$g_{45}$	1.106144793719	0.050277183440
20-S5	1/16	$g_{12}$	2.059638006775	0.102643784933	197-S7	1/24	$g_{14}$	-0.128843563571	-0.003942067525
21-S5	1/24	$g_4$	-0.213590327764	-0.003731682713	198-S7	1/16	$g_{52}$	0.815707802129	0.032877730545
22-S5	1/4	$g_{11}$	1.177687787771	0.051418670702	199-S7	1/4	$g_{43}$	0.635702829750	0.025518064643
23-S5	1/2	$g_{10}$	1.093576383486	0.049451372165	200-S7	1/16	$g_{45}$	1.106144793719	0.050277183440
24-S5	1/8	$g_{11}$	0.944371175125	0.032955416087	201-S7	1/24	$g_{15}$	-0.113126023891	-0.003290535327
25-S5	1/2	$g_{10}$	0.734587686279	0.025567072553	202-S7	1/16	$g_{52}$	1.342508904936	0.071390284829
26-S5	1/6	$g_5$	0.47723573065*	0.01715756028	203-S7	1/12	$g_{15}$	-0.096261106599	-0.003155179167
27-M6	1/16	$g_{13}$	0.092703296625	0	204-S7	1/16	$g_{53}$	0.942042143809	0.050485695523
28-M6	1/12	$g_{13}$	0.062064397151	0	205-S7	1/4	$g_{42}$	0.664812550858	0.032801749909
29-M6	1/32	$g_{14}$	-0.032433915322	0	206-S7	1/8	$g_{47}$	0.746247163126	0.036654897006
30-M6	1/8	$g_{15}$	-0.558960605344	0	207-S7	1/144	$g_{13}$	0.015400329826	0.000164624707
31-M6	1/16	$g_{15}$	-0.406156736719	0	208-S7	1/96	$g_{14}$	-0.148081924590	-0.003305011557
32-M6	1/4	$g_{16}$	-0.316465247271	0	209-S7	1/48	$g_{13}$	0.015548592044	0.000160182577
33-M6	1/24	$g_{13}$	0.045271743432	0	210-S7	1/32	$g_{40}$	-0.363469627011	-0.004727828507
34-M6	1/48	$g_{13}$	0.070805748949	0	211-S7	1/16	$g_{38}$	-0.31134215536	-0.00404674919
35-M6	1/4	$g_{16}$	-0.535115380809	0	212-S7	1/8	$g_{42}$	0.81924717224	0.046855489196
36-M6	1/8	$g_{15}$	-0.831785654370	0	213-S7	1/24	$g_{15}$	-0.112542632056	-0.003478053745
37-M6	1/8	$g_{16}$	-0.667694545359	0	214-S7	1/8	$g_{47}$	0.91405093408	0.04486160082
38-M6	1/12	$g_9$	-0.21440337147	0	215-S7	1/8	$g_{54}$	0.828736871089	0.040880626848
39-S6	1/24	$g_7$	0.025334411533	0.000134151236	216-S7	1/8	$g_{46}$	0.95215768567	0.04559036202
40-S6	1/16	$g_8$	-0.512249210261	-0.003730210466	217-S7	1/4	$g_{42}$	0.59759777279	0.02595026422
41-S6	1/8	$g_9$	-0.271221697673	-0.001890072089	218-S7	1/8	$g_{53}$	0.774920557284	0.033638518217
42-S6	1/72	$g_7$	0.021623868322	0.000141394973	219-S7	1/32	$g_{40}$	-0.246180375270	-0.004550733992
43-S6	1/8	$g_9$	-0.43846576066	-0.00319405093	220-S7	1/8	$g_{43}$	0.961197181072	0.046855489196
44-S6	1/4	$g_{17}$	-0.259325943995	-0.004300120594	221-S7	1/16	$g_{38}$	-0.188790327282	-0.002374789360
45-S6	1/6	$g_9$	-0.119009992648	-0.003308367453	222-S7	1/4	$g_{42}$	0.58123025452	0.02495949785
46-S6	1/4	$g_{18}$	0.879291241521	0.047113097898	223-S7	1/4	$g_{55}$	0.35733921887	0.01511183749
47-S6	1/4	$g_{19}$	1.120968561756	0.059552411259	224-S7	1/16	$g_{40}$	-0.200696579093	-0.004500005469
48-S6	1/8	$g_{20}$	1.542237652030	0.080253512938	225-S7	1/12	$g_{15}$	-0.065174820497	-0.001839165015
49-S6	1/8	$g_{21}$	1.176947197512	0.062822045769	226-S7	1/16	$g_{52}$	0.702185354197	0.023943701788
50-S6	1/12	$g_9$	-0.140199070719	-0.003403733352	227-S7	1/8	$g_{47}$	0.407663379492	0.013494432296
51-S6	1/4	$g_{21}$	0.865925201214	0.040831704607	228-S7	1/12	$g_{15}$	-0.08195863410	-0.00211512505
52-S6	1/2	$g_{18}$	0.782731311849	0.037539120424	229-S7	1/4	$g_{53}$	0.490372577726	0.016658394455
53-S6	1/12	$g_8$	-0.147488212902	-0.003907983810	230-S7	1/2	$g_{42}$	0.36993498100	0.01245375453
54-S6	1/32	$g_{22}$	2.044600225603	0.101571794444	231-S7	1/12	$g_{15}$	-0.08195863410	-0.00211512505
55-S6	1/8	$g_{20}$	1.137071072414	0.051222861796	232-S7	1/2	$g_{42}$	0.36993498100	0.01245375453





130-M7	1/16	$g_{37}$	-0.494415425222	0	307-S7	1/36	$g_{13}$	0.010485980621	0.000143949321
131-M7	1/4	$g_{36}$	-0.41989663865	0	308-S7	1/4	$g_{41}$	0.27709244190*	0.00746928985
132-M7	1/8	$g_{34}$	-0.542017150796	0	309-S7	1/12	$g_{15}$	-0.072993670101	-0.001976781189
133-M7	1/4	$g_{38}$	-0.2010875739**	0	310-S7	1/8	$g_{47}$	0.54154753559	0.01945547104
134-M7	1/32	$g_{30}$	0.057209654200	0	311-S7	1/2	$g_{44}$	0.41728030634	0.01494610501
135-M7	1/16	$g_{35}$	-0.65804614052	0	312-S7	1/16	$g_{46}$	0.607654217590	0.025416236198
136-M7	1/8	$g_{36}$	-0.49327378592	0	313-S7	1/6	$g_{16}$	-0.05189612468	-0.00105446532
137-M7	1/96	$g_{28}$	0.069176047800	0	314-S7	1/2	$g_{48}$	0.30611471184	0.00872378220
138-M7	1/16	$g_{36}$	-0.491439771**	0	315-S7	1/8	$g_{54}$	0.416000342949	0.012096422783
139-M7	1/32	$g_{33}$	-0.800600314818	0	316-S7	1/1	$g_{56}$	0.17349841526	0.00475514760
140-M7	1/8	$g_{38}$	-0.15678153586	0	317-S7	1/2	$g_{57}$	0.17914799102	0.00497574659
141-M7	1/48	$g_{29}$	0.038380451088	0	318-S7	1/2	$g_{59}$	0.12223230107	0.00332646474
142-M7	1/4	$g_{38}$	-0.16148138890	0	319-S7	1/24	$g_{13}$	0.023539759080	0.000168392224
143-M7	1/8	$g_{36}$	-0.35422809760	0	320-S7	1/8	$g_{42}$	0.39745790655	0.01134906488
144-M7	1/4	$g_{39}$	-0.11081591890	0	321-S7	1/2	$g_{41}$	0.29746997541	0.00837896648
145-S7	1/16	$g_{13}$	0.036278976466	0.000158781404	322-S7	1/8	$g_{50}$	0.35097358861	0.01003156199
146-S7	1/12	$g_{14}$	0.028592826473	0.000147520009	323-S7	1/4	$g_{58}$	0.11200684(65)	0.002934044(22)
147-S7	1/32	$g_{13}$	-0.562933518492	-0.003584909865	324-S7	1/6	$g_{16}$	-0.066786319580	-0.001901654937
148-S7	1/8	$g_{15}$	-0.297654173362	-0.001836208735	325-S7	1/4	$g_{44}$	0.532227035472	0.023800456805
149-S7	1/16	$g_{15}$	-0.207555228859	-0.001215771810	326-S7	1/4	$g_{41}$	0.471398155593	0.021205531919
150-S7	1/4	$g_{16}$	-0.161644383198	-0.000945042482	327-S7	1/16	$g_{38}$	-0.143600626236	-0.002341515026
151-S7	1/24	$g_{13}$	0.028711924535	0.000168339233	328-S7	1/2	$g_{41}$	0.40256253226	0.01541675510
152-S7	1/48	$g_{13}$	0.031801483472	0.000155670095	329-S7	1/2	$g_{49}$	0.2408938124**	0.0091028154*
153-S7	1/4	$g_{16}$	-0.28664763500	-0.00177064771	330-S7	1/4	$g_{42}$	0.53011891513	0.02052915892
154-S7	1/8	$g_{15}$	-0.45651280619	-0.00291467186	331-S7	1/2	$g_{41}$	0.40699861908	0.01578213619
155-S7	1/8	$g_{16}$	-0.36721882223	-0.00234684076	332-S7	1/6	$g_9$	-0.03327128907*	-0.00071484464
156-S7	1/12	$g_9$	-0.1101540890**	-0.00064080576	333-S7	1/12	$g_9$	-0.03233713444	-0.00074619804
157-S7	1/12	$g_{13}$	0.013391408702	0.000160623702	334-S7	1/1	$g_{49}$	0.19856030714	0.00601526961
158-S7	1/8	$g_{40}$	-0.300396192752	-0.004260505313	335-S7	1/1	$g_{60}$	0.11669921848	0.00353726638
159-S7	1/4	$g_{38}$	-0.156922345580	-0.002172374372	336-S7	1/1	$g_{59}$	0.17040027980	0.00516337873
160-S7	1/36	$g_{13}$	0.012817474926	0.000165556889	337-S7	1/4	$g_{55}$	0.27313504687	0.00842786560
161-S7	1/4	$g_{38}$	-0.25729167687	-0.00364837451	338-S7	1/2	$g_{59}$	0.17869340447	0.00559074588
162-S7	1/4	$g_{38}$	-0.160550866158	-0.003782129544	339-S7	1/4	$g_{57}$	0.26110837786	0.00835316544
163-S7	1/6	$g_{16}$	-0.075881836191	-0.002524110547	340-S7	1/2	$g_{25}$	0.11163367834	0.00333921861
164-S7	1/4	$g_{41}$	0.572724291583	0.031135889252	341-S7	1/2	$g_{58}$	0.16178590989	0.00485764945
165-S7	1/4	$g_{42}$	0.733711248698	0.039635195293	342-S7	1/12	$g_{16}$	-0.052565424208	-0.000929056468
166-S7	1/8	$g_{43}$	1.033924815474	0.054881037579	343-S7	1/4	$g_{56}$	0.25493509530	0.00810369020
167-S7	1/4	$g_{44}$	0.782547139439	0.042410572712	344-S7	1/2	$g_{56}$	0.24870245765	0.00779831998
168-S7	1/12	$g_{16}$	-0.089380432289	-0.002665803419	345-S7	1/8	$g_{55}$	0.26307959329	0.00791848968
169-S7	1/4	$g_{44}$	0.576651527776	0.028328751343	346-S7	1/4	$g_{49}$	0.19864889227	0.00603498255
170-S7	1/2	$g_{41}$	0.516195727537	0.025716040464	347-S7	1/2	$g_{58}$	0.16748684(75)	0.005145002(32)
171-S7	1/12	$g_{15}$	-0.099385135580	-0.003196017365	348-S7	1/4	$g_{49}$	0.18925230589	0.00553447373
172-S7	1/16	$g_{45}$	1.494759772685	0.077174394769	349-S7	1/1	$g_{60}$	0.11070332(35)	0.003243273(14)
173-S7	1/8	$g_{46}$	0.822000194835	0.039293990833	350-S7	1/2	$g_{59}$	0.17193262172	0.00525283507
174-S7	1/8	$g_{47}$	1.011972832768	0.054702376849	351-S7	1/48	$g_{15}$	-0.067427158448	-0.001192271595
175-S7	1/24	$g_{15}$	-0.115595929722	-0.003026809384	352-S7	1/8	$g_{57}$	0.24582805220	0.00758817302
176-S7	1/8	$g_{38}$	-0.196626012265	-0.004116199520	353-S7	1/12	$g_{25}$	0.10201073910	0.00287693468
177-S7	1/4	$g_{44}$	0.721067216848	0.035832522650					

TABLE IX: Group factors  $g_n$  for Table VIII.

$n$	$g_n$	$n$	$g_n$
1	$(2+N)/3$	31	$(2+N)^2(112+80N+40N^2+10N^3+N^4)/2187$
2	$(2+N)^2/9$	32	$(2+N)^2(136+80N+24N^2+3N^3)/2187$
3	$(2+N)(8+N)/27$	33	$(2+N)^2(144+80N+18N^2+N^3)/2187$
4	$(2+N)^2(8+N)/81$	34	$(2+N)^2(152+76N+14N^2+N^3)/2187$
5	$(2+N)(22+5N)/81$	35	$(2+N)^2(156+76N+11N^2)/2187$
6	$(2+N)(20+6N+N^2)/81$	36	$(2+N)^2(164+72N+7N^2)/2187$
7	$(2+N)^3/27$	37	$(2+N)^2(160+72N+10N^2+N^3)/2187$
8	$(2+N)^2(20+6N+N^2)/243$	38	$(2+N)^2(8+N)(22+5N)/2187$
9	$(2+N)^2(22+5N)/243$	39	$(2+N)^2(186+55N+2N^2)/2187$
10	$(2+N)(60+20N+N^2)/243$	40	$(2+N)^2(8+N)(20+6N+N^2)/2187$
11	$(2+N)(56+22N+3N^2)/243$	41	$(2+N)(448+244N+36N^2+N^3)/2187$
12	$(2+N)(48+24N+8N^2+N^3)/243$	42	$(2+N)(416+252N+56N^2+5N^3)/2187$
13	$(2+N)^3(8+N)/243$	43	$(2+N)(368+256N+88N^2+16N^3+N^4)/2187$
14	$(2+N)^2(48+24N+8N^2+N^3)/729$	44	$(2+N)(424+252N+50N^2+3N^3)/2187$
15	$(2+N)^2(56+22N+3N^2)/729$	45	$(2+N)(320+256N+120N^2+30N^3+3N^4)/2187$
16	$(2+N)^2(60+20N+N^2)/729$	46	$(2+N)(384+260N+76N^2+9N^3)/2187$
17	$(2+N)^2(8+N)^2/729$	47	$(2+N)(400+260N+64N^2+5N^3)/2187$
18	$(2+N)(164+72N+7N^2)/729$	48	$(2+N)(440+244N+42N^2+3N^3)/2187$

19	$(2+N)(152+76N+14N^2+N^3)/729$	49	$(2+N)(22+5N)^2/2187$
20	$(2+N)(136+80N+24N^2+3N^3)/729$	50	$(2+N)(432+252N+44N^2+N^3)/2187$
21	$(2+N)(156+76N+11N^2)/729$	51	$(2+N)(256+240N+160N^2+60N^3+12N^4+N^5)/2187$
22	$(2+N)(112+80N+40N^2+10N^3+N^4)/729$	52	$(2+N)(352+264N+96N^2+16N^3+N^4)/2187$
23	$(2+N)(144+80N+18N^2+N^3)/729$	53	$(2+N)(384+256N+76N^2+12N^3+N^4)/2187$
24	$(2+N)(160+72N+10N^2+N^3)/729$	54	$(2+N)(400+248N+68N^2+12N^3+N^4)/2187$
25	$(2+N)(8+N)(22+5N)/729$	55	$(2+N)(22+5N)(20+6N+N^2)/2187$
26	$(2+N)(186+55N+2N^2)/729$	56	$(2+N)(472+224N+32N^2+N^3)/2187$
27	$(2+N)^4/81$	57	$(2+N)(464+224N+38N^2+3N^3)/2187$
28	$(2+N)^3(20+6N+N^2)/729$	58	$(2+N)(504+206N+19N^2)/2187$
29	$(2+N)^3(22+5N)/729$	59	$(2+N)(492+210N+26N^2+N^3)/2187$
30	$(2+N)^3(8+N)^2/2187$	60	$(2+N)(526+189N+14N^2)/2187$

- [1] M.H. Anderson, J.R. Ensher, M.R. Matthews, C. Wieman, and E.A. Cornell, *Science* **269**, 198 (1995); K.B. Davis, M.O. Mewes, M.R. Andrews, N.J. van Druten, D.S. Durfee, D.M. Kurn, and W. Ketterle, *Phys. Rev. Lett.* **75**, 3969 (1995); C.C. Bradley, C.A. Sackett, J.J. Tollett, and R.G. Hulet, *Phys. Rev. Lett.* **75**, 1687 (1995).
- [2] G. Baym, J.-P. Blaizot, M. Holzmann, F. Laloë, and D. Vautherin, *Phys. Rev. Lett.* **83**, 1703 (1999) [cond-mat/9905430].
- [3] G. Baym, J.-P. Blaizot, and J. Zinn-Justin, *Europhys. Lett.* **49**, 150 (2000) [cond-mat/9907241].
- [4] M. Holzmann, G. Baym, J.-P. Blaizot, and F. Laloë, *Phys. Rev. Lett.* **87**, 120403 (2001) [cond-mat/0103595].
- [5] J.O. Andersen, *Rev. Mod. Phys.*, to be published [cond-mat/0305138v2].
- [6] S. Giorgini, L.P. Pitaevskii, and S. Stringari, *Phys. Rev. A* **54**, R4633 (1996).
- [7] P. Arnold and B. Tomášik, *Phys. Rev. A* **64**, 053609 (2001) [cond-mat/0105147].
- [8] P. Arnold, G. Moore, and B. Tomášik, *Phys. Rev. A* **65**, 013606 (2001) [cond-mat/0107124].
- [9] K. Huang and C.N. Yang, *Phys. Rev.* **105**, 767 (1957); K. Huang, C.N. Yang, and J.M. Luttinger, *Phys. Rev.* **105**, 776 (1957).
- [10] X. Sun, *Phys. Rev. E* **67**, 066702 (2003) [hep-lat/0209144].
- [11] B. Kastening, *Phys. Rev. A* **68**, 061601(R) (2003) [cond-mat/0303486].
- [12] B. Kastening, *Phys. Rev. A* **69**, 043613 (2004) [cond-mat/0309060].
- [13] B. Kastening, *Laser Phys.* **14**, 586 (2004) [cond-mat/0404354].
- [14] The quantity actually considered in [12, 13] is  $c_1 = \alpha\kappa_N$ , where  $\alpha = -256\pi^3/[\zeta(3/2)]^{4/3} \approx -2206.19$ .
- [15] V.A. Kashurnikov, N.V. Prokof'ev, and B.V. Svistunov, *Phys. Rev. Lett.* **87**, 120402 (2001) [cond-mat/0103149]; N.V. Prokof'ev and B.V. Svistunov, *Phys. Rev. Lett.* **87**, 160601 (2001) [cond-mat/0103146].
- [16] P. Arnold and G. Moore, *Phys. Rev. Lett.* **87**, 120401 (2001) [cond-mat/0103228].
- [17] P. Arnold and G. Moore, *Phys. Rev. E* **64**, 066113 (2001) [cond-mat/0103227].
- [18] H. Kleinert and V. Schulte-Frohlinde, *Critical Properties of  $\phi^4$ -Theories*, 1st ed. (World Scientific, Singapore, 2001).
- [19] P. Arnold and B. Tomášik, *Phys. Rev. A* **62**, 063604 (2000) [cond-mat/0005197].
- [20] H. Kleinert, A. Pelster, B. Kastening, and M. Bachmann, *Phys. Rev. E* **62**, 1537 (2000) [hep-th/9907168]; B. Kastening, *Phys. Rev. E* **61**, 3501 (2000) [hep-th/9908172].
- [21] D.B. Murray and B.G. Nickel, Univ. of Guelph Report, 1991, unpublished.
- [22] M. Muthukumar and B. Nickel, *J. Chem. Phys.* **80**, 5839 (1984).
- [23] F. Wegner, *Phys. Rev. B* **5**, 4529 (1972).
- [24] J. Zinn-Justin, *Quantum Field Theory and Critical Phenomena*, 4th ed. (Clarendon, Oxford, 2002); A. Pelissetto and E. Vicari, *Phys. Rev.* **368**, 549 (2002) [cond-mat/0012164].
- [25] B. Hamprecht and H. Kleinert, *Phys. Rev. D* **68**, 065001 (2003) [hep-th/0302116].
- [26] H. Kleinert, *Phys. Lett. A* **207**, 133 (1995) [quant-ph/9507005].
- [27] H. Kleinert, *Phys. Rev. D* **57**, 2264 (1998); *Phys. Rev. D* **58**, 107702 (1998) [cond-mat/9803268].
- [28] H. Kleinert, *Phys. Rev. D* **60**, 085001 (1999) [hep-th/9812197]; *Phys. Lett. A* **277**, 205 (2000) [cond-mat/9906107].
- [29] H. Kleinert, *Path Integrals in Quantum Mechanics, Statistics and Polymer Physics*, 3rd ed. (World Scientific, Singapore, 2004).
- [30] V.I. Yukalov, *Moscow Univ. Phys. Bull.* **31**, 10 (1976).
- [31] H. Kleinert and B. Van den Bossche, *Phys. Rev. E* **63**, 056113 (2001) [cond-mat/0011329].
- [32] P.M. Stevenson, *Phys. Rev. D* **23**, 2916 (1981).
- [33] F.F. de Souza Cruz, M.B. Pinto, R.O. Ramos, and P. Sena, *Phys. Rev. A* **65**, 053613 (2002) [cond-mat/0112306].
- [34] J.-L. Kneur, A. Neveu, and M.B. Pinto, *Phys. Rev. A* **69**, 053624 (2004) [cond-mat/0401324].
- [35] The connection between the coefficients  $A_l$  of [34] and our coefficients for  $N = 2$ , given in Eqs. (30) and Table III, is  $A_2 = 4b'_2$ ,  $A_3 = -16b_3$ ,  $A_4 = 64b_4$ ,  $A_5 = -256b_5$ . Their values  $A_4 = 3.57259 \times 10^{-6}$  and  $A_5 = 2.25332 \times 10^{-7}$  should, according to our results, read  $A_4 = 3.46941 \times 10^{-6}$  and  $A_5 = 2.23296 \times 10^{-7}$ . With the conventions of [34], the constant under the logarithm, quoted in [34] as  $-0.59775$ , should read  $\frac{1}{2} - \ln 3 \approx -0.598612$ .
- [36] B.G. Nickel, D.I. Meiron, and G.A. Baker, Jr., Univ. of Guelph Report, 1977, unpublished.
- [37] J.F. Nagle, *J. Math. Phys.* **7**, 1588 (1966).